TARGETED DELETION OF JUN/AP-1 IN ALVEOLAR EPITHELIAL CELLS CAUSES PROGRESSIVE EMPHYSEMA AND WORSENS CIGARETTE SMOKE-INDUCED LUNG INFLAMMATION

Narsa M. Reddy[1*], Suryanaraya Vegiraju[1], Ashley Irving[1], Bogdan C Paun[1], Irina G Luzina[2], Sergei P Atamas[2], Shyam Biswal[1], Navas-Acien Ana[1], Wayne Mitzner[1] and Sekhar P. Reddy[1*$]

[1] Department of Environmental Health Sciences, Johns Hopkins Bloomberg School of Public Health, Baltimore, MD 21205

[2] Department of Medicine, University of Maryland School of Medicine and Baltimore VA Medical Center, Baltimore, MD, USA.

* Present address: Department of Pediatrics, University of Illinois at Chicago

$To whom all correspondence should be addressed:

Sekhar P. Reddy, PhD, Department of Pediatrics, University of Illinois at Chicago

840 S Wood Street, Chicago, IL 60612

Chicago, IL 60612; Tel: 312-413-3606: Email: sreddy03@uic.edu

Running Title: Protective role of c-Jun in lung emphysema

Abstract

The c-Jun/AP-1 transcriptional factor is known to regulate cell proliferation, apoptosis, and inflammatory responses; however its role in lung pathogenesis is largely unknown. Here we report that the declined expression levels of c-Jun mRNA and protein in the lung tissues of advanced chronic obstructive pulmonary disease (COPD) patients, and that genetic deletion of c-Jun specifically in alveolar epithelial cells causes progressive emphysema with lung inflammation and alveolar air space enlargement, which are cardinal features of emphysema. Although mice lacking *c-Jun* specifically in lung alveolar epithelial cells appear normal at 6 weeks of age, when exposed to chronic cigarette smoke, *c-Jun* mutant mice display more lung inflammation with perivascular and peribronchiolar infiltrates. These results demonstrate that the c-Jun/AP-1 pathway is critical for maintaining lung alveolar cell homeostasis and that loss of its expression can contribute to lung inflammation and progressive emphysema.

Introduction

COPD is projected to be the third-leading cause of death worldwide by 2020.[1, 2] COPD is a chronic lung disease characterized by severely impaired normal lung function. The development of COPD appears to occur slowly and progressively over many years, as it is generally diagnosed in middle-aged or older individuals.[2] Exposure to cigarette smoke is a major risk factor for the development of COPD.[3] Only a subset of cigarette smokers develop COPD and other factors such as air pollution and infections also contribute to its pathogenesis suggests that both genetic factors and environmental modifiers contribute to the development of COPD.[4] Although the mechanisms underlying the development and progression of this disease remain enigmatic, histopathologic examination of the lungs of patients with severe COPD has revealed a severe loss of lung tissue, especially of the alveolar type II cells, and persistent lung inflammation (reviewed in).[5] Data obtained from molecular and cellular analyses of lung tissue samples from COPD patients and from experimental mouse models of emphysema have suggested critical roles for deregulated cell proliferation, antioxidant-oxidant imbalance, and apoptosis as well as degradation of the extracellular matrix in COPD.[6]

The activator protein 1 (AP-1), comprised of the c-Jun (c-Jun, Jun-B, and Jun-D) and Fos (Fos, Fos-B, Fra-1, and Fra-2) families of DNA binding proteins, binds to the TPA response element (TRE, TGAC/GTCA) and regulates the expression of genes involved in various biological processes including cell proliferation, differentiation, cell death, inflammation, and cellular defense.[7] Various cellular processes controlled by the AP-1 transcriptional factor have been reported to be deregulated in lung tissue/cell types obtained from COPD patients.[5] Although the members of the AP-1 family of proteins are activated in response to various insults in lung epithelial cells,[8] whether the activation of AP-1 proteins is critical to confer protection on the host or to enhance the host's

susceptibility to the development and progression of lung diseases is still largely undefined in vivo. Thus, in the present study, we have examined the role of c-Jun/AP-1 transcription factors in COPD. First, we determined the expression levels of this transcription factor in COPD clinical samples and found the loss of c-Jun expression in the lung tissues obtained from very severe-COPD patients (GOLD stage IV) when compared to control non-COPD individuals. Since conventional deletion of *c-Jun* results in embryonic lethality,[9] we utilized a mouse model in which *c-Jun* was specifically deleted in type II alveolar epithelial cells. We then examined the effects of c-Jun deficiency on both lung development and on cigarette smoke-induced lung inflammation and tissue destruction in these mice. Here, we report for the first time that the c-Jun deficiency in alveolar type II epithelial cells results in progressive emphysema and also perpetuates cigarette smoke-induced lung inflammation in vivo.

Materials and Methods

Human lung tissue samples: Lung tissue samples used in this study were obtained from the Lung Tissue Research Consortium funded by the NHLBI. One tissue sample was obtained from each subject; i.e. 'n' represents the number subjects in this study. Patients' lung function data were obtained from established patient registries. The subjects were classified as per severity of COPD according to the guidelines of the Global Initiative for Obstructive Lung Disease (GOLD). The non-COPD population (21 samples with 15 former smokers, 1 current smoker and 6 never smokers) had normal lung function performance and no evidence of COPD (Table 1). Groups for COPD lungs included GOLD-II, GOLD-III and GOLD-IV on the basis of lung function tests. Clinical and demographical characters of these patients are presented in Table 1.

Mice: Mice carrying the floxed *c-Jun* allele (hereafter referred to as *c-Jun*$^{f/f}$) were generated on C57BL/6x129SVJ background as described elsewhere.[10] Mice expressing Cre recombinase under the control of *SP-C* promoter on C57BL/6 background were obtained from Dr. Brigid Hogan, Duke University.[11] Wild type mice with C57BL6x129SVJ background were used as additional controls in selective experiments. To generate the mice with c-Jun deletion in alveolar type II epithelial cells, *c-Jun*$^{f/f}$ mice were crossed with SPC-Cre mice ("see Supplemental Figure S1A at http://ajp.amjpathol.org"). The resulting *c-Jun*$^{f/wt}$*-SPC-Cre* mice were backcrossed to the parental *c-Jun*$^{f/f}$ mice to obtain *c-Jun*$^{f/f}$*- SPC-Cre* mice (hereafter referred to as *c-Jun*$^{\Delta ae}$). All animal protocols were performed in accordance with guidelines approved by the animal care and use committee at the Johns Hopkins University.

PCR genotyping and determination c-Jun deletion in alveolar epithelial cells: We used Jun1: CTCATACCAGTTCGCACAGGCGGC (Forward) and Jun2: CCGCTAGCACTCACGTTGGTAGGC (Reverse) primers for the detection of 'floxed' alleles. For the detection of SPC-Cre, SPC: GACACATATAAGACCCTGGTCA (forward) and Cre: ACGAACCTGGTCGAAATC AGTGCG (reverse) primers were used as outlined ("see Supplemental Figure S1B at http://ajp.amjpathol.org"). Alveolar type II epithelial cells were isolated and cultured as described previously.[12] For the detection of *c-Jun* deletion in lung epithelium, the genomic DNA from type II epithelial cells was amplified using Jun1 and Jun3 (CAGGGCGTTGTGTCA CTGAGCT, reverse) primers ("see Supplemental Diagram S1B at http://ajp.amjpathol.org").

Cigarette smoke exposure: Mice (8-week old) were divided into two groups: control and cigarette smoke exposure groups. Control groups were housed in a filtered air environment. Experimental groups were subjected to cigarette smoke exposure for 5

h/day, 5 days/week for 6 months using whole- body smoke exposure system (Model TE-10,Teague Enterprises, CA) using 2R4F reference cigarettes with 2.45 mg nicotine per cigarette (Tobacco Research Institute, University of Kentucky, KY) as described elsewhere.[13] Each smoldering cigarette was puffed for 2 seconds, once every minute for a total of 8 puffs, at a flow rate of 1.05 l/min, to provide a standard puff of 35 cm3.The smoke machine was adjusted to produce a mixture of side stream smoke (89%) and mainstream smoke (11%) by burning five cigarettes at one time. Chamber atmosphere was monitored for total suspended particles and carbon monoxide, with concentrations of 90 mg/m3 and 350 ppm, respectively.

Lung morphology measurements: Lung morphometric measurements were performed as described previously.[14, 15] Mice were anesthetized with sodium pentobarbital and lungs were inflated with warmed (50–55°C) 0.8% low-melt agarose in 1.5% paraformaldehyde at 25–30 cm H_2O. The inflation pressure was measured continuously until the agarose started to gel (~ 1 min). The whole animal was placed in a refrigerator at 4°C for 30 min. The cooled agarose-filled lungs were excised and placed in 1.5% paraformaldehyde for 24 h at 4°C. Lung tissues were washed in distilled water and placed in 70% ethyl alcohol. Before histological sectioning, the left lung was dissected, and the inferior and superior 3mm along the long axis of the lung was removed. The remaining tissue was cut into three 2- to 3-mm-thick sections, and embedded in paraffin. Five-micrometer-thick sections were cut and stained with H & E. The slides were coded and representative images (15 per lung section) were acquired with Nikon Digital Camera DXM1200 (Nikon, Tokyo, Japan) at 100x magnification. Mean chord length (MCL) were measured using ImageJ software (NIH, Bethesda, MD) and by computer-assisted morphometry with Image Pro Plus software with sampling grid lines 17 μm apart ensuring one to two chords per alveolus. Arteries, veins, or bronchioles were avoided in morphometric measurements.

Terminal Deoxynucleotidyl Transferase dUTP Nick End Labeling (TUNEL) Assay: DNA damage was assessed using In Situ Cell Death Detection Kit (Roche Applied Science, Indianapolis, IN) as per manufacturer's instructions. Briefly, the lung tissue sections were deparaffinized, washed with PBS, blocked with 3% H_2O_2 in methanol, permeabilized, and then incubated with 50 μl of TUNEL mixture for 1 h at 37°C. The sections were analyzed under fluorescent microscope and images were captured. The number of TUNEL-positive cells in tissue sections (10 fields/lung section) was counted and expressed as mean ± SEM.

Assessment of lung inflammation: Mice were anesthetized, tracheas cannulated and lungs were lavaged twice with 1ml of cold PBS. Cells from the bronchoalveolar lavage (BAL) fluid were centrifuged, and total inflammatory cells were counted using hemocytometer. Differential cell counts were determined by staining with Diff-Quick Stain Set (Dade-Behring, Newark, DE). For each sample, 300 cells (macrophages, neutrophils and lymphocytes) were counted based on standard cytological criteria.

Cytokine analysis: BAL fluid samples from mice were analyzed by the multiplex suspension array system using Luminex beads (Bio-Rad Laboratories, Hercules, CA), which included the following cytokines: IL1β, IL1α, IL2, IL3, IL4, IL5, IL6, IL9, IL10, IL12p40, IL12p70, IL13, IL17, eotaxin, GCSF, GMCSF, IFNγ, MCP1, MIP1α, MIP1β, RANTES and TNFα. BAL samples of different age groups were thawed, diluted 1:1 with diluent, and ran according to the manufacturer's protocol and measured as picograms per milliliter of BAL fluid (n=3-5).

Real-time RT-PCR: Total RNA was isolated from lungs of *c-Jun*$^{f/f}$ and *c-Jun*$^{\Delta ae}$ mice and lung tissues of human non-COPD, moderate-COPD, severe-COPD and very severe - COPD patients using RNeasy kit (Qiagen, Germantown, MD) and reverse transcribed with superscript first strand cDNA synthesis system (Invitrogen, Carlsbad, CA). Real-time RT-PCRs were performed using Taqman gene expression assays specific for mouse *Gclc, Nqo1,* and *Hmox1* and human *c-JUN*. For the detection of *SPA, SPC* and *SPD* expression, we used sybr green 1 dye reagent (Applied Biosystems, Carlsbad, CA) and gene specific primer sets. For *SPA*, CAGTGTGATTGGGAGAAACC (forward) and TGTCTCCATGTTCTCCAGGT (reverse) primers; for *SPC*, CAAAGAGGTCCTGATGGAGA (forward), TCATACACAACGATGCCAGT (reverse), for *SPD*, GGCTGCTTTCC TGAGTATGA (forward) and GGCAACATACAGGTCTGAGC (reverse), for *β-actin*, CTA CAATGAGCTGCGTGTGGC (forward) and CGAACAATTTCCCTCTCAGC (reverse) primers were used. The absolute expression values for each gene were normalized to that of actin and values from 1.5 month old *c-Jun*$^{\Delta ae}$ mice samples were set as one unit. Fold changes for c-JUN expression in COPD samples were calculated by setting the lowest c-Jun expression sample as one unit.

Western blot analysis: Non-COPD and severe-COPD and very severe - COPD lung tissues were homogenized, and protein concentrations were estimated using BCA reagent (Thermo Scientific, Rockford, IL). Equal amounts of protein were separated and immunoblotted with anti-c-JUN antibodies (Santa Cruz Biotechnology, Santa Cruz, CA). The blots were developed with the ECL Western blot detection system (Thermo Scientific, Rockford, IL). Bands were quantified using β-actin as reference.

Immunohistochemistry: Immunohistochemical staining on human COPD lung tissue

sections and on lung tissue sections of *c-Jun*$^{f/f}$ and *c-Jun*$^{\Delta ae}$ mice exposed to cigarette smoke was performed as previously reported.[16] Briefly, tissue slides were deparaffinized and rehydrated. After antigen recovery with DakoCytomation Target Retrieval Solution, pH 9, for 20 min in a microwave oven, non-specific binding was blocked with 3% BSA solution. Immunohistochemical staining was performed with anti-c-JUN (Santa Cruz Biotechnology, Santa Cruz, CA) or anti-B220 (BD Biosciences, Franklin Lakes, NJ) or anti-CD3 (Daco, Carpinteria, CA) antibodies. Staining was visualized with Dako Universal LSAB horseradish peroxidase kit, following manufacturer's recommendations.

Statistical Analysis: All data involving COPD samples (Non-COPD, moderate-COPD, severe COPD and very severe COPD (n=88 for *c-JUN* mRNA analysis and n=36 for *c-*JUN protein analyses) were described by median and interquartile range and scatter plots. We compared the relative expression levels of c-JUN mRNA and protein in lung tissue samples from individuals with moderate-COPD, severe-COPD and very severe-COPD to non-COPD control samples, our main comparison, using linear regression models without any adjustment and with further adjustment for sex, age and cigarette pack-years. We also used Bonferroni correction for multiple comparisons.
All animal data were expressed as the mean ± SEM (n = 8 for each condition). One-way ANOVA followed by Newman-Kuels post hoc analysis was performed for multiple comparisons. *P* values with $\leq$ 0.05 were considered as statistically significant. For comparing the interaction between age and emphysema, two-way ANOVA with a Bonferroni correction was used. A Bonferroni-corrected *P* value of $\leq$ 0.05 was used to identify statistical significance.

RESULTS

Deregulation of c-JUN expression in COPD lung tissues

To determine whether *c-JUN* expression is dysregulated with the progression of emphysema in humans, we measured the expression levels of *c-JUN* mRNA and protein in non-COPD (FEV1 > 80%, GOLD-0/GOLD-1), moderate COPD (FEV ≤ 50-80%, GOLD II) severe COPD (FEV1 ≤ 30-50%, GOLD-III), and very severe COPD (FEV1 < 30% GOLD-IV) lung tissue samples. Clinical and demographic characteristics of the COPD patients are given in Table 1. Compared to non-COPD lung tissue samples, *c-JUN* mRNA levels were significantly decreased in very severe-COPD lungs (0.45 fold lower, $P = 0.008$) but not in moderate- (0.88 fold lower, $P = 0.58$) and severe-COPD lungs (0.66 fold lower, $P = 0.19$) (Figure 1A). The decreased *c-JUN* mRNA levels comparing very severe-COPD to non-COPD lung tissue were similar after adjustment for age, sex and pack-year ($P = 0.009$). Using Bonferroni corrections for multiple comparisons, the only difference was between the very-severe and non-COPD lung tissues ($P = 0.05$). Consistent with this result, c-JUN protein levels, as assessed by western blot analysis, were lower in homogenates of very severe-COPD lung tissue as compared to the non-COPD control tissue samples (0.29 fold, $P = 0.001$) or moderate-COPD samples (0.26 fold, $P = 0.001$), but no differences were observed for severe-COPD lung tissue (Figure 1B). After adjustment for age, gender and cigarette pack years the lower c-JUN protein levels were statistically significant in the severe-COPD ($P = 0.026$) and very severe-COPD ($P = 0.001$) group. The c-JUN protein levels were significantly lower in very severe-COPD lung tissues than in non-COPD or moderate-COPD lung tissues when compared using Bonferroni corrections for multiple comparisons ($P < 0.001$). We next evaluated c-JUN expression in the intact tissues by immunohistochemistry. Consistent with results obtained from mRNA and protein expression data, immunohistochemical analysis of COPD and non-COPD lung tissue sections with c-JUN antibodies revealed

decreased levels of c-JUN-positive cells in severe- and very severe COPD tissues when compared to control non-COPD and moderate-COPD tissue sections (P = 0.001 with Bonferroni corrections for multiple comparisons)(Figure 1C). The c-JUN expression was highly detectable mainly in epithelial cells in non-COPD and moderate-COPD lung tissues, but its expression was gradually decreased in severe-COPD and very severe-COPD tissues. These results suggest that loss of c-JUN may contribute to the development and/or progression of emphysema.

Genetic deletion of *c-Jun* in the alveolar epithelium

To determine whether loss of c-Jun contributed to emphysema *in vivo*, we have deleted c-Jun in mouse lung epithelium by conditionally gene targeting approach. The mice bearing *c-Jun* "floxed" allele (*c-Jun*$^{f/f}$ mice) were crossed with mice bearing Cre recombinase cDNA under the control of a surfactant protein C (SPC) promoter.[11] To determine *c-Jun* deletion in these mice, *c-Jun*$^{f/f}$ and *c-Jun*$^{\Delta ae}$ mice were genotyped for the presence of the *Cre* gene and *c-Jun* floxed alleles, as outlined in Supplemental Figure S1B at http://ajp.amjpathol.org". We observed both deleted and undeleted *c-Jun* floxed alleles in the total lung tissue of *c-Jun*$^{\Delta ae}$ mice ("See Supplemental Figure S1C, lane 3, left panel at http://ajp.amjpathol.org"), because Cre expressed under the control of the SPC promoter mainly deletes c-Jun in type II alveolar epithelial cells and not in other lung cell types.[17] To further confirm the deletion, type II cells were isolated from the lungs of *c-Jun*$^{f/f}$ and *c-Jun*$^{\Delta ae}$ mice, and genomic DNA was amplified. As anticipated, PCR amplified a high molecular weight deletion band (520 bp) but not the floxed allele band (320 bp) in *c-Jun*$^{\Delta ae}$ cells ("See Supplemental Figure S1C, right panel at http://ajp.amjpathol.org"). These results confirmed that *c-Jun* was specifically deleted from the type II epithelial cells of *c-Jun*$^{\Delta ae}$ mice.

Genetic disruption of *c-Jun* in the alveolar epithelium leads to progressive emphysema

To determine whether *c-Jun* deletion affects the lung development, *c-Jun*$^{\Delta ae}$ mice and Cre- negative *c-Jun*$^{f/f}$ littermates were sacrificed at 1.5, 3, 8, or 12 months of age. Histological assessment of lungs from *c-Jun*$^{\Delta ae}$ and *c-Jun*$^{f/f}$ littermates revealed no apparent abnormalities at the microscopic level at 6 weeks of age (Figure 2A). However, histologic examination of the lungs revealed abnormalities such as enlarged air spaces and infiltration of atypical foamy alveolar macrophages in 3-month-old *c-Jun* mutant mice; this phenotype was not detectable in their wild-type (*c-Jun*$^{f/f}$) littermates. The presence of foamy alveolar macrophages was persisted in the lungs of *c-Jun*$^{\Delta ae}$ mice up to 8 months of age. A significant degree of alveolar space enlargement was observed in the lungs of the 8-month-old *c-Jun*$^{\Delta ae}$ mice, and this was even greater in the 12-month age group ("See Supplemental Figure S2 for 40x and 100x images at http://ajp.amjpathol.org"). However, as can be appreciated in the low power (40x) images in Figure 2A, the nature of this pathologic development was quite heterogeneous, with localized destruction leading to large cavities in the parenchyma. In contrast, this striking emphysematous phenotype was not seen either in *c-Jun*$^{f/f}$ mice (Figure 2A) or in wild type mice ("See Supplemental Figure S2 at http://ajp.amjpathol.org") or wild type mice bearing SPC-Cre recombinase ("See Supplemental Figure S3 at http://ajp.amjpathol.org").

To determine the magnitude of the emphysema caused by *c-Jun* deletion, we measured the MCL using computer-assisted morphometry analysis (Figure 2B). The increase in the MCL generally indicates airspace (alveolar size) enlargement and greater severity of emphysema.[18, 19] The MCL of the *c-Jun* mutant mice at 1.5 months of age was not

different from that of wild type mice (Figure 2B). However, the chord lengths of the *c-Jun*$^{\Delta ae}$ mice were increased by 15% and 17% when compared to *c-Jun*$^{f/f}$ mice at 3 and 8 months of age, respectively. There was a dramatic increase in the lung tissue damage and the MCL in *c-Jun*$^{\Delta ae}$ mice by 39% at 12 months of age. The MCL of *c-Jun*$^{f/f}$ mice lungs increased by 22% at 3 months of age when compared to that of 1.5-month-old mice, but it remained stable at this level through 12 months of age. To determine whether Cre recombinase expression has any effect on the integrity of the lung structure, lungs from wild type mice expressing Cre recombinase under the control of *SPC* promoter were harvested at 12 months of age. There was no noticeable defect in lung structure in these mice as evaluated by histopathology and MCL quantification. Histopathology and MCL in these mice were comparable to that of mice with *c-Jun* floxed allele (*c-Jun*$^{f/f}$ mice) ("See Supplemental Figure S3 at http://ajp.amjpathol.org"). Although it would have been best to calculate alveolar surface area, we unfortunately did not measure the lung volumes. However, neither the simple MCL nor a calculated surface area will reflect the extreme heterogeneity of the tissue destruction as seen in Figure 2A. Nevertheless, there is clearly progressive destruction of alveolar tissue in the *c-Jun*$^{\Delta ae}$ mice, suggesting a prominent role for c-Jun in the proper maintenance of lung alveolar cell homeostasis in adult mice, and deregulation of c-Jun expression in alveolar epithelial cells can promote emphysema severity with age.

Deletion of *c-Jun* in the alveolar epithelium causes DNA damage in the lung

Several studies have reported the presence of endothelial and epithelial apoptosis in lungs of COPD patients and in experimental models of COPD.[20] In order to determine whether deletion of *c-Jun* from alveolar type II epithelial cells induces emphysema via cellular apoptosis in the lungs, we performed TUNEL assays on lung sections of *c-Jun*$^{f/f}$ and *c-Jun*$^{\Delta ae}$ mice (Figure 3). As shown in Figure 3A, low levels of TUNEL-positive cells

were present in the lungs of *c-Jun*$^{\Delta ae}$ mice (~ 3 cells per field) at 1.5 months of age, but none in *c-Jun*$^{f/f}$ mice. The number of TUNEL-positive cells gradually increased in 3- and 8-month-old *c-Jun*$^{\Delta ae}$ mice by 7.5 and 31 cells per field, respectively (Figure 3B). This increase in the number of TUNEL-positive cells was consistent with the increase in the severity of the lung damage and emphysema in *c-Jun* mutant mice. In 12-month-old *c-Jun*$^{\Delta ae}$ mice, the number of TUNEL-positive cells declined to 20 per field, as compared to 8-month age old littermates. In contrast to the situation in *c-Jun* mutant mice, there were very few apoptotic cells (1-2 per field) in the lungs of all age groups of *c-Jun*$^{f/f}$ mice. These results suggest that loss of c-Jun expression in alveolar epithelium results in elevated levels of cellular apoptosis, there by leading to progressive loss of alveolar epithelium.

The c-Jun deficiency deregulates antioxidant enzyme and inflammatory cytokine expression

Deregulation of antioxidant gene expression has been implicated in lung tissue destruction leading to emphysema.[5, 21] Therefore, we asked whether c-Jun deficiency would decrease antioxidant gene expression, leading to increased levels of lung cell apoptosis. To answer this question, we analyzed the expression levels of representative antioxidant enzymes, Gclc, Nqo1, and Hmox1. We chose these enzymes as they play roles in cellular detoxification and maintenance of redox status and are also transcriptionally regulated by AP-1 transcription factor. [5, 21] Gene expression analysis revealed deregulated expression of *Gclc,* Nqo1 and Hmox1 in the lungs of *c-Jun* mutant mice as compared to the littermate control group (Figure 4A). The mRNA expression levels of all three enzymes were significantly lower in 3-month-old *c-Jun* mutant mice than in wild type mice, but their expression levels between these two genotypes in 8-month age groups were not different statistically. The expression levels of *Nqo1* and

Hmox1, but not *Gclc*, were significantly lower in 12-month-old *c-Jun* mutant mice than in wild type mice (Figure 4A). These results suggest that a lack of the c-Jun/AP-1 pathway alters the response to cellular stress, at least, in part, as a result of deregulation of antioxidant gene expression.

A number of cytokines have been shown to play a role in the orchestration of inflammation in COPD by activating, recruiting, and prolonging the survival of inflammatory cells.[6] We therefore assessed the levels of several cytokines and chemokines in the BAL fluid of *c-Jun*$^{\Delta ae}$ and *c-Jun*$^{f/f}$ mice using multiplex cytokine assays. Of the cytokines measured, only the levels of four, TNFα, IL12p40, IL13, and CXCL1, and showed a significant difference in between *c-Jun*$^{\Delta ae}$ mice and their *c-Jun*$^{f/f}$ littermates (Figure 4B). BAL fluids from the 3- and 8-month age groups of *c-Jun*$^{\Delta ae}$ mice had elevated levels of TNFα when compared to those of their counterpart *c-Jun*$^{f/f}$ littermates. IL12p40 levels were not different between the genotypes at 3 months of age, but they were markedly higher in 8-month-old *c-Jun*$^{\Delta ae}$ mice (83 pg/ml) than *c-Jun*$^{f/f}$ mice (8 pg/ml). In mutant mice, although not statistically significant, IL12p40 levels were still higher (14 pg/ml) than those in *c-Jun*$^{f/f}$ mice (8 pg/ml) at 12 months of age. Similarly, levels of Cxcl1 (KC or human IL-8 equivalent) were significantly elevated in *c-Jun* mutant mice at 3 and 12 months of age, when compared to wild type mice (Figure 4B). Likewise, IL13 levels were also not different between the two genotypes in 3 month and 12 month age groups but significantly elevated in *c-Jun*$^{\Delta ae}$ mice in 8-month age groups compared to their *c-Jun*$^{f/f}$ littermates (Figure 4B).

Prolonged exposure to cigarette smoke induces perivascular and peribronchiolar inflammation in *c-Jun* mutant mice

Because cigarette smoke is a major etiological factor in the pathogenesis of COPD and inflammation, we asked whether *c-Jun* deletion in alveolar epithelial cells increases the severity of the lung pathogenesis in response to cigarette smoke exposure. We exposed *c-Jun*$^{f/f}$ and *c-Jun*$^{\Delta ae}$ (8-week-old) mice to cigarette smoke for 6 months (as detailed in the Methods section) and then assessed lung inflammation and tissue damage. Lung inflammation and air space enlargement were assessed by inflammatory cell analysis in the BAL fluid and by measuring the MCL of lung tissue sections, respectively. We found elevated numbers of inflammatory cells, mainly consisting of neutrophils, macrophages, and lymphocytes, in the lungs of *c-Jun* mutant mice as compared to *c-Jun*$^{f/f}$ mice (Figure 5A). The percent increase in total neutrophils in the BAL of cigarette smoke-exposed *c-Jun*$^{\Delta ae}$ mice over room air controls was 20-fold greater than those in their *c-Jun*$^{f/f}$ counterparts (200% vs. 10% in *c-Jun*$^{\Delta ae}$ compared to *c-Jun*$^{f/f}$ mice*)*. Likewise, epithelial cell sloughing was 1.7-fold higher in *c-Jun*$^{\Delta ae}$ mice as compared with their *c-Jun*$^{f/f}$ counterparts (125% vs. 70%, *c-Jun*$^{\Delta ae}$ vs. *c-Jun*$^{f/f}$ mice). However, percent increase in total cells (36% vs. 37% % in c-*Jun*$^{\Delta ae}$ vs. *c-Jun*$^{f/f}$ *mice*) and macrophages (32% vs. 36%, *Jun*$^{\Delta ae}$ vs. *c-Jun*$^{f/f}$ mice) was not statistically different between the two genotypes following smoke exposure. Histopathologic examination revealed the lymphocyte infiltrates adjacent to the blood vessels and airways in the lungs of *c-Jun*$^{\Delta ae}$ mice exposed to cigarette smoke (Figure 5B; "See Supplemental Figure S4 for 40x images at http://ajp.amjpathol.org") that resembled the bronchus associated lymphoid tissue (BALT) phenotype observed in the lung tissue of COPD patients.[22] We then used morphometry to quantify the effects of c-Jun deficiency on lung tissue destruction. As expected, the MCL in lungs of cigarette smoke-exposed *c-Jun*$^{f/f}$ mice was greater than that in the filtered room air-exposed control group (Figure 5C). However, cigarette smoke exposure did not alter the magnitude of emphysema caused by the deletion of *c-Jun* (Figure 5C). The average MCLs of cigarette smoke-exposed *c-Jun*$^{\Delta ae}$ mice were comparable to those of room air-exposed *c-Jun*$^{\Delta ae}$ mice. These results strongly

support a prominent role for c-Jun in the proper maintenance of lung alveolar cell homeostasis and in reducing the lung inflammation induced by cigarette smoke.

We further identified the cell types infiltrating the perivascular and peribronchiolar regions of the lungs of *c-Jun* mutant mice by immunostaining the lung tissue sections with the anti-CD3 and anti-B220 antibodies, which specifically stain T-lymphocytes and B-lymphocytes, respectively. Immunostaining revealed that the perivascular and peribronchial infiltrates in the lungs of *c-Jun*$^{\Delta ae}$ mice consisted mainly of T- (Figure 5D) and B-lymphocytes (Figure 5E). This type of immune infiltration was not seen in the lungs of cigarette smoke-exposed *c-Jun*$^{f/f}$ mice or in the lungs of filter air-exposed control mice of either genotype.

DISCUSSION

Our current findings demonstrate for the first time a critical role for the c-Jun/AP-1-pathway in maintaining lung alveolar epithelial cell homeostasis by reducing cellular stress and inflammation. The continual progression of emphysema (e.g., the destruction of alveoli and persistent inflammation) in *c-Jun*$^{\Delta ae}$ mice is akin to the pace of emphysema that develops in smokers. Consistent with this observation, we found a substantial loss of c-JUN expression in the lung tissues obtained from patients with severe COPD symptoms when compared to non-COPD patients (Figure 1). Importantly, the lack of the c-Jun transcription factor enhanced the severity of cigarette smoke-induced lung inflammation with lymphocyte infiltrates, which are observed in the lungs of COPD patients.[22] In contrast, a specific deletion of *c-Jun* in Clara cells did not cause progressive emphysema in mice data not shown) nor was any such phenotype detectable in wild-type mice with Cre recombinase at up to 12 months of age ("See Supplemental Figure S3 at http://ajp.amjpathol.org"). Thus, it appears that a loss of *c-Jun* expression specifically in the alveolar epithelium may enhance susceptibility to the development and progression of emphysema.

COPD is characterized by chronic bronchitis and emphysema. Various experimental models of emphysema have been used to elucidate the mechanisms underlying the pathogenesis of COPD. One of these models, cigarette smoke, has been widely used because it utilizes the relevant etiological agent that causes COPD. We and others have shown that chronic exposure to cigarette smoke in the mouse displays several of the characteristic hallmarks of COPD, including airspace enlargement, oxidative stress, apoptosis, inflammation, and protease-anti-protease imbalance.[13, 23] One of the limitations of the chronic cigarette smoke model, however, is the mild degree of emphysema it produces. Several studies have utilized other non-smoking models, such as the instillation of elastase,[24, 25] VEGF inhibition,[26, 27] caspase 3 instillation,[28] and ceramide activation.[29] These models have the advantage of causing airspace enlargement in a shorter period of time (cigarette smoke exposure requires 6 months), and they are also known to induce lung inflammation and cellular apoptosis, which lead to airspace enlargement. However, although there are limitations associated with using chronic cigarette smoke exposure in mice (such as a lack of chronic bronchitis because of undetectable levels of mucus production), this model has been considered the most relevant model for COPD research because it uses the etiologic agent that causes the majority of COPD cases.

Both alveolar epithelial and endothelial cell apoptosis and proliferation are known to be deregulated in the lungs of rodents exposed to experimental emphysema,[6] as well as in the lungs of patients with emphysema COPD.[20] This phenotype has been generally attributed to elevated levels of oxidative stress, and protease-anti-protease imbalance caused by the impact of cigarette smoke on lung structural cells and of infiltrated leukocytes.[5, 30, 31] Consistent with this notion, targeted deletion of *c-Jun* in type II epithelial cells gradually increased the level of apoptosis (as assessed by TUNEL-positive staining) in the lungs at

1.5 to 8 months of age, and the number of apoptotic cells gradually increased with age (Figure 3). This apoptotic cell death was accompanied by an inflammatory response at 3 months of age, leading to a gradual loss of lung alveoli in 8- and 12-month-old mice (Figure 2A). Although apoptosis gradually increased up to 8 months of age in c-*Jun*$^{\Delta ae}$ mice, the MCL remained at the level of 3-month-old mice. The decrease in TUNEL staining at 12 months of age could be attributed to the loss of alveolar epithelium in the lung, as reflected in the histopathology and MCL (Figure 2). It is likely that the lung epithelium switches from apoptosis to necrotic cell death in *c-Jun* mutant mice between the ages of 8 and 12 months, reflecting a change in the aging process. Indeed, this change is consistent with the presence of fewer apoptotic cells in these mice at the later time. From 3 to 8 months, apoptosis may be the predominant mechanism of cell elimination (*versus* necrosis) because of the absence of c-Jun signaling. Since apoptosis generally does not drive inflammation, a lesser MCL effect is seen during the initial phase. This balance changes over time to favor necrosis. Thus, the loss of c-Jun, combined with an increase in the age of the mice, leads to a rise in necrosis over apoptosis as well as the promotion of tissue destruction and the inflammatory responses commonly seen in emphysema. Also supporting this contention is a previous report that cigarette smoke exposure induces necrosis by inhibiting apoptosis in lung epithelial cells.[32] Decreased levels of CD46 complementary regulatory protein, which regulates T-regulatory cell turnover, are associated with a loss of lung function and the development of emphysema in COPD patients, and depletion of CD46 in an experimental model of emphysema has been reported to promote the necrosis of inflammatory cells, rather than apoptosis.[33]

Increased level of apoptosis was accompanied by decreased expression of several antioxidant enzymes such as Gclc, Nqo1 and Hmox1 in the lungs of c-Jun mutant mice (Figure 4A). Previously, it was shown that c-Jun regulates the expression of Nqo1 and Gclc

by transcriptional activation of ARE elements on their promoters by associating with Nrf2[34] and Hmox1 through the induction of Fos/AP-1 activity.[35] Also, mouse embryonic fibroblasts deficient in c-Jun undergo premature senescence due to proliferation defects caused by increased level of spontaneous DNA damage and impaired repair.[36-39] Furthermore, the c-Jun/AP-1 transcription factor is a critical regulator of cell proliferation and survival. For example, the lack of c-Jun impairs liver cell generation mainly due to increased cell death of hepatocytes.[10] c-Jun promotes the survival of hepatocytes by regulating the expression of inducible nitric oxide synthase and total nitric oxide levels in experimental hepatitis.[40] Thus, lack of the c-Jun transcription factor in alveolar epithelium likely results in deregulation of cellular redox state that may contribute to DNA damage, leading to the impairment of epithelial cell regeneration and emphysema.

Inflammation is a common feature in the pathogenesis of many chronic conditions, including COPD/emphysema.[21] Multiple cytokines orchestrate the recruitment and activation of inflammatory cells and thereby contribute to both acute and chronic airway diseases such as COPD.[41] In the present study, we found increased levels of a pro-inflammatory cytokine TNFα in BAL fluids obtain from 3- and 8-month-old *c-Jun* mutant mice as compared to wild type mice. TNFα has been implicated in emphysema. For example, increased levels of TNFα has been observed in COPD patients[42] and in cigarette smoke-induced experimental emphysema.[43] c-Jun has been shown to regulate the TNFα levels through regulating the expression of tissue inhibitor of metalloproteinase 3 (TIMP3),[44] a potent inhibitor of TNFα converting enzyme (TACE). Conditional and inducible deletion of both *c-Jun* and *Jun-B* in the epidermis of adult mice developed psoriasis-like inflammatory skin disease.[45] Analysis of skin lesions in these double mutant mice revealed a remarkable increase in the inflammatory cells consisting of T- lymphocytes and inflammatory cytokines such as TNFα,

IL12p40, MIP1, and MIP2.[45] We also found increased levels of IL13, Cxcl1, and IL12p40, in c-Jun mutant mice (Figure 4B). Lung specific expression of IL13 promoted the development of emphysema and inflammation,[46] whereas Cxcl1 possesses neutrophil chemoattractant activity and IL12p40 regulates immune responses.[47] Thus, it is likely that a deregulated 21 cytokine expression resulting from lack of the c-Jun/AP-1 signaling in the alveolar epithelium contributes to the progression of emphysema.

We noted a persistent presence of foamy (atypical) alveolar macrophages in *c-Jun*$^{\Delta ae}$ mice, which was correlated with the lung tissue damage and progression of emphysema. Consistent with this observation, the presence of foamy (hypertrophic) alveolar macrophages was noted in several experimental models of emphysema. For example, genetic disruption of surfactant protein D (SPD) causes progressive emphysema accompanied by the hypertrophic alveolar macrophages in the lung[48, 49] Gene expression analysis revealed strikingly lower levels of *SPA*, *SPC* and *SPD* in the lungs of *c-Jun*$^{\Delta ae}$ mice when compared to their *c-Jun*$^{f/f}$ counterparts ("See Supplemental Figure S5 at http://ajp.amjpathol.org"). The fact that *c-Jun*$^{\Delta ae}$ mice exhibited progressive emphysema analogous to that in *SPD*$^{-/-}$ mice and that AP-1 is known to regulate *SPD* expression[50] strongly support our contention that deregulation of c-Jun/AP-1-regulated surfactant gene expression may contribute in part to the progression of emphysema. In addition, both gradual and age-related emphysema have been observed in mouse models lacking β-subunit of αvβ6 integrin,[51] lysosomal acid lipase,[52] NADPH oxidase,[30] TLR4 and MyD88,[53] and placental growth factor.[54] Whether c-Jun acts as a functional effector in mediating cellular functions and maintaining the lung tissue homeostasis regulated by these proteins remains to be investigated in our experimental conditions. COPD is characterized by an inflammatory response by the lungs to inhaled substances such as cigarette smoke and airborne pollutants. Cigarette smoke induces both humoral and cell-mediated immune

responses via the release and inhibition of both pro- and anti-inflammatory cytokines.[55] Deletion of *c-Jun* leads to severe inflammation, consisting of T- and B-lymphocyte accumulation around the major airways and blood vessels in the lung (Figure 5) following cigarette smoke exposure. To our knowledge, this is first report that c-Jun deficiency enhances the severity of lung inflammation with perivascular and peribronchial lymphocyte infiltration. Moreover, we have found that c-JUN expression is decreased in lung tissue samples from patients with severe- or very severe-COPD, as compared to those without COPD. Therefore, we now propose that the loss of *c-Jun* expression in alveolar epithelium may be a susceptibility factor underlying cigarette smoke-induced lung inflammation and emphysema development. Paradoxically, c-JUN is highly expressed in human lung cancer tissues/cells, and its expression is correlated with a poor prognosis in lung cancer patients.[56-59] However, transgenic overexpression of c-Jun alone in mice does not lead to an overt phenotype in all most all tissues, including the lung.[60] On the contrary, overexpression of this transcription factor in hamster tracheal epithelial cells induces their proliferation and transformation in vitro,[61] and transgenic expression of a mutant form of c-Jun in the lung epithelial cells inhibits carcinogen induced lung tumorigenesis.[62] The pro-carcinogenic effects of c-Jun in chemically and viral induced pathogenesis are mainly attributed to its pro-proliferative and anti-apoptotic effects, mediated by the upregulation of cell cycle genes and suppression p53-mediated functions, respectively [7]. Although c-Jun has procarcinogenic effects, lack of its pro-proliferative and anti-apoptotic effects may be contributing to the loss of lung tissue in *c-Jun*$^{\Delta ae}$ mice that are seen under our experimental conditions. Whether the activation of this transcription factor may prove a useful new strategy for treating COPD or this approach may be problematic because it could have potential pro-carcinogenic effects warrants further investigation.

ACKNOWLEDGMENTS

This work was funded by National Institute of Health grants: RO1-ES11863, RO1-HL66109 and RO3-HL96933 (to SPR), the Flight Attendant Medical Research Institute CIA-award (to SPR), and the NIEHS training grant ES007141 (to SV). We thank both Pathology Core of the ALI-SCCOR (P50-HL073994) and COPD-SCCOR (P50-HL084945) supported by Hopkins-NIEHS center for utilizing their facilities and services in the present study. We also thank Dr. Erwin Wagner for proving *c-Jun*$^{f/f}$ mice and Dr. Brigid Hogan for providing SPC-Cre mice.

REFERENCES

1. Murray CJ, Lopez AD: Alternative projections of mortality and disability by cause 1990-2020: Global Burden of Disease Study. Lancet 1997, 349:1498-1504
2. National Institute of Health NH, Lung and Blood Institute Morbidity and mortality:. 2009 chartbook on cardiovascular,lung, and blood diseases. Edited by NIH.
3. Buist AS, McBurnie MA, Vollmer WM, Gillespie S, Burney P, Mannino DM, Menezes AM, Sullivan SD, Lee TA, Weiss KB, Jensen RL, Marks GB, Gulsvik A, Nizankowska-Mogilnicka E: International variation in the prevalence of COPD (the BOLD Study): a population-based prevalence study. Lancet 2007, 370:741-750
4. DeMeo DL, Hersh CP, Hoffman EA, Litonjua AA, Lazarus R, Sparrow D, Benditt JO, Criner G, Make B, Martinez FJ, Scanlon PD, Sciurba FC, Utz JP, Reilly JJ, Silverman EK: Genetic determinants of emphysema distribution in the national emphysema treatment trial. Am J Respir Crit Care Med 2007, 176:42-48
5. Yoshida T, Tuder RM: Pathobiology of cigarette smoke-induced chronic obstructive pulmonary disease. Physiol Rev 2007, 87:1047-1082
6. Barnes PJ: Mediators of chronic obstructive pulmonary disease. Pharmacol Rev 2004, 56:515-548
7. Eferl R, Wagner EF: AP-1: a double-edged sword in tumorigenesis. Nat Rev Cancer 2003, 3:859-868
8. Reddy SP, Mossman BT: Role and regulation of activator protein-1 in toxicant-induced responses of the lung. Am J Physiol Lung Cell Mol Physiol 2002, 283:L1161-1178
9. Hilberg F, Aguzzi A, Howells N, Wagner EF: c-jun is essential for normal mouse development and hepatogenesis. Nature 1993, 365:179-181

10. Behrens A, Sibilia M, David JP, Mohle-Steinlein U, Tronche F, Schutz G, Wagner EF: Impaired postnatal hepatocyte proliferation and liver regeneration in mice lacking c-jun in the liver. EMBO J 2002, 21:1782-1790
11. Eblaghie MC, Reedy M, Oliver T, Mishina Y, Hogan BL: Evidence that autocrine signaling through Bmpr1a regulates the proliferation, survival and morphogenetic behavior of distal lung epithelial cells. Dev Biol 2006, 291:67-82
12. Reddy NM, Kleeberger SR, Cho HY, Yamamoto M, Kensler TW, Biswal S, Reddy SP: Deficiency in Nrf2-GSH signaling impairs type II cell growth and enhances sensitivity to oxidants. Am J Respir Cell Mol Biol 2007, 37:3-8
13. Rangasamy T, Cho CY, Thimmulappa RK, Zhen L, Srisuma SS, Kensler TW, Yamamoto M, Petrache I, Tuder RM, Biswal S: Genetic ablation of Nrf2 enhances susceptibility to cigarette smoke-induced emphysema in mice. J Clin Invest 2004, 114:1248-1259
14. Bishai JM, Mitzner W, Tankersley CG, Wagner EM: PEEP-induced changes in epithelial permeability in inbred mouse strains. Respir Physiol Neurobiol 2007, 156:340-344
15. Bishai JM, Mitzner W: Effect of severe calorie restriction on the lung in two strains of mice. Am J Physiol Lung Cell Mol Physiol 2008, 295:L356-362
16. Luzina IG, Todd NW, Nacu N, Lockatell V, Choi J, Hummers LK, Atamas SP: Regulation of pulmonary inflammation and fibrosis through expression of integrins alphaVbeta3 and alphaVbeta5 on pulmonary T lymphocytes. Arthritis Rheum 2009, 60:1530-1539
17. Okubo T, Hogan BL: Hyperactive Wnt signaling changes the developmental potential of embryonic lung endoderm. J Biol 2004, 3:11

18. Shim YM, Zhu Z, Zheng T, Lee CG, Homer RJ, Ma B, Elias JA: Role of 5-lipoxygenase in IL-13-induced pulmonary inflammation and remodeling. J Immunol 2006, 177:1918-1924

19. Wang Z, Zheng T, Zhu Z, Homer RJ, Riese RJ, Chapman HA, Jr., Shapiro SD, Elias JA: Interferon gamma induction of pulmonary emphysema in the adult murine lung. J Exp Med 2000, 192:1587-1600

20. Morissette MC, Parent J, Milot J: Alveolar epithelial and endothelial cell apoptosis in emphysema: what we know and what we need to know. Int J Chron Obstruct Pulmon Dis 2009, 4:19-31

21. Macnee W: Pathogenesis of chronic obstructive pulmonary disease. Clin Chest Med 2007, 28:479-513

22. Hogg JC, Chu F, Utokaparch S, Woods R, Elliott WM, Buzatu L, Cherniack RM, Rogers RM, Sciurba FC, Coxson HO, Pare PD: The nature of small-airway obstruction in chronic obstructive pulmonary disease. N Engl J Med 2004, 350:2645-2653

23. Hautamaki RD, Kobayashi DK, Senior RM, Shapiro SD: Requirement for macrophage elastase for cigarette smoke-induced emphysema in mice. Science 1997, 277:2002-2004.

24. Qian SY, Mitzner W: In vivo and in vitro lung reactivity in elastase-induced emphysema in hamsters. Am Rev Respir Dis 1989, 140:1549-1555

25. Hantos Z, Adamicza A, Janosi TZ, Szabari MV, Tolnai J, Suki B: Lung volumes and respiratory mechanics in elastase-induced emphysema in mice. J Appl Physiol 2008, 105:1864-1872

26. Marwick JA, Stevenson CS, Giddings J, MacNee W, Butler K, Rahman I, Kirkham PA: Cigarette smoke disrupts VEGF165-VEGFR-2 receptor signaling complex in rat lungs

and patients with COPD: morphological impact of VEGFR-2 inhibition. Am J Physiol Lung Cell Mol Physiol 2006, 290:L897-908

27. Edirisinghe I, Yang SR, Yao H, Rajendrasozhan S, Caito S, Adenuga D, Wong C, Rahman A, Phipps RP, Jin ZG, Rahman I: VEGFR-2 inhibition augments cigarette smoke-induced oxidative stress and inflammatory responses leading to endothelial dysfunction. FASEB J 2008, 22:2297-2310
28. Aoshiba K, Yokohori N, Nagai A: Alveolar wall apoptosis causes lung destruction and emphysematous changes. Am J Respir Cell Mol Biol 2003, 28:555-562
29. Petrache I, Natarajan V, Zhen L, Medler TR, Richter AT, Cho C, Hubbard WC, Berdyshev EV, Tuder RM: Ceramide upregulation causes pulmonary cell apoptosis and emphysema-like disease in mice. Nat Med 2005, 11:491-498
30. Kassim SY, Fu X, Liles WC, Shapiro SD, Parks WC, Heinecke JW: NADPH oxidase restrains the matrix metalloproteinase activity of macrophages. J Biol Chem 2005, 280:30201-30205
31. Yokohori N, Aoshiba K, Nagai A: Increased levels of cell death and proliferation in alveolar wall cells in patients with pulmonary emphysema. Chest 2004, 125:626-632
32. Wickenden JA, Clarke MC, Rossi AG, Rahman I, Faux SP, Donaldson K, MacNee W: Cigarette smoke prevents apoptosis through inhibition of caspase activation and induces necrosis. Am J Respir Cell Mol Biol 2003, 29:562-570
33. Grumelli S, Lu B, Peterson L, Maeno T, Gerard C: CD46 protects against chronic obstructive pulmonary disease. PLoS ONE 6:e18785

34. Jeyapaul J, Jaiswal AK: Nrf2 and c-Jun regulation of antioxidant response element (ARE)-mediated expression and induction of gamma-glutamylcysteine synthetase heavy subunit gene. Biochem Pharmacol 2000, 59:1433-1439

35. Hsieh HL, Wang HH, Wu CY, Yang CM: Reactive Oxygen Species-Dependent c-Fos/Activator Protein 1 Induction Upregulates Heme Oxygenase-1 Expression by Bradykinin in Brain Astrocytes. Antioxid Redox Signal 13:1829-1844

36. Johnson RS, van Lingen B, Papaioannou VE, Spiegelman BM: A null mutation at the c-jun locus causes embryonic lethality and retarded cell growth in culture. Genes Dev 1993, 7:1309-1317

37. Schreiber M, Kolbus A, Piu F, Szabowski A, Mohle-Steinlein U, Tian J, Karin M, Angel P, Wagner EF: Control of cell cycle progression by c-Jun is p53 dependent. Genes Dev 1999, 13:607-619

38. Wisdom R, Johnson RS, Moore C: c-Jun regulates cell cycle progression and apoptosis by distinct mechanisms. EMBO J 1999, 18:188-197

39. MacLaren A, Black EJ, Clark W, Gillespie DA: c-Jun-deficient cells undergo premature senescence as a result of spontaneous DNA damage accumulation. Mol Cell Biol 2004, 24:9006-9018

40. Hasselblatt P, Rath M, Komnenovic V, Zatloukal K, Wagner EF: Hepatocyte survival in acute hepatitis is due to c-Jun/AP-1-dependent expression of inducible nitric oxide synthase. Proc Natl Acad Sci U S A 2007, 104:17105-17110

41. Churg A, Cosio M, Wright JL: Mechanisms of cigarette smoke-induced COPD: insights from animal models. Am J Physiol Lung Cell Mol Physiol 2008, 294:L612-631

42. Pitsiou G, Kyriazis G, Hatzizisi O, Argyropoulou P, Mavrofridis E, Patakas D: Tumor necrosis factor-alpha serum levels, weight loss and tissue oxygenation in chronic obstructive pulmonary disease. Respir Med 2002, 96:594-598

43. Churg A, Wang RD, Tai H, Wang X, Xie C, Wright JL: Tumor necrosis factor-alpha drives 70% of cigarette smoke-induced emphysema in the mouse. Am J Respir Crit Care Med 2004, 170:492-498

44. Guinea-Viniegra J, Zenz R, Scheuch H, Hnisz D, Holcmann M, Bakiri L, Schonthaler HB, Sibilia M, Wagner EF: TNFalpha shedding and epidermal inflammation are controlled by Jun proteins. Genes Dev 2009, 23:2663-2674

45. Zenz R, Eferl R, Kenner L, Florin L, Hummerich L, Mehic D, Scheuch H, Angel P, Tschachler E, Wagner EF: Psoriasis-like skin disease and arthritis caused by inducible epidermal deletion of Jun proteins. Nature 2005, 437:369-375

46. Zheng T, Zhu Z, Wang Z, Homer RJ, Ma B, Riese RJ, Jr., Chapman HA, Jr., Shapiro SD, Elias JA: Inducible targeting of IL-13 to the adult lung causes matrix metalloproteinase- and cathepsin-dependent emphysema. J Clin Invest 2000, 106:1081-1093

47. Kato K, Shimozato O, Hoshi K, Wakimoto H, Hamada H, Yagita H, Okumura K: Local production of the p40 subunit of interleukin 12 suppresses T-helper 1-mediated immune responses and prevents allogeneic myoblast rejection. Proc Natl Acad Sci U S A 1996, 93:9085-9089

48. Wert S, Jones T, Korfhagen T, Fisher J, Whitsett J: Spontaneous emphysema in surfactant protein D gene-targeted mice. Chest 2000, 117:248S

49. Korfhagen TR, Sheftelyevich V, Burhans MS, Bruno MD, Ross GF, Wert SE, Stahlman MT, Jobe AH, Ikegami M, Whitsett JA, Fisher JH: Surfactant protein-D regulates surfactant phospholipid homeostasis in vivo. J Biol Chem 1998, 273:28438-28443

50. He Y, Crouch EC, Rust K, Spaite E, Brody SL: Proximal promoter of the surfactant protein D gene: regulatory roles of AP-1, forkhead box, and GT box binding proteins. J Biol Chem 2000, 275:31051-31060.

51. Morris DG, Huang X, Kaminski N, Wang Y, Shapiro SD, Dolganov G, Glick A, Sheppard D: Loss of integrin alpha(v)beta6-mediated TGF-beta activation causes Mmp12-dependent emphysema. Nature 2003, 422:169-173

52. Lian X, Yan C, Yang L, Xu Y, Du H: Lysosomal acid lipase deficiency causes respiratory inflammation and destruction in the lung. Am J Physiol Lung Cell Mol Physiol 2004, 286:L801-807

53. Zhang X, Shan P, Jiang G, Cohn L, Lee PJ: Toll-like receptor 4 deficiency causes pulmonary emphysema. J Clin Invest 2006, 116:3050-3059

54. Tsao PN, Su YN, Li H, Huang PH, Chien CT, Lai YL, Lee CN, Chen CA, Cheng WF, Wei SC, Yu CJ, Hsieh FJ, Hsu SM: Overexpression of placenta growth factor contributes to the pathogenesis of pulmonary emphysema. Am J Respir Crit Care Med 2004, 169:505-511

55. Cornwell WD, Kim V, Song C, Rogers TJ: Pathogenesis of inflammation and repair in advanced COPD. Semin Respir Crit Care Med 31:257-266

56. Wodrich W, Volm M: Overexpression of oncoproteins in non-small cell lung carcinomas of smokers. Carcinogenesis 1993, 14:1121-1124

57. Szabo E, Riffe ME, Steinberg SM, Birrer MJ, Linnoila RI: Altered cJUN expression: an early event in human lung carcinogenesis. Cancer Res 1996, 56:305-315

58. Volm M, Rittgen W, Drings P: Prognostic value of ERBB-1, VEGF, cyclin A, FOS, JUN and MYC in patients with squamous cell lung carcinomas. Br J Cancer 1998, 77:663-669

59. Volm M, Koomagi R, Mattern J, Efferth T: Expression profile of genes in non-small cell lung carcinomas from long-term surviving patients. Clin Cancer Res 2002, 8:1843-1848

60. Grigoriadis AE, Schellander K, Wang ZQ, Wagner EF: Osteoblasts are target cells for transformation in c-fos transgenic mice. J Cell Biol 1993, 122:685-701.

61. Timblin CR, Janssen YW, Mossman BT: Transcriptional activation of the proto-oncogene c-jun by asbestos and H2O2 is directly related to increased proliferation and transformation of tracheal epithelial cells. Cancer Res 1995, 55:2723-2726.

62. Tichelaar JW, Yan Y, Tan Q, Wang Y, Estensen RD, Young MR, Colburn NH, Yin H, Goodin C, Anderson MW, You M: A dominant-negative c-jun mutant inhibits lung carcinogenesis in mice. Cancer Prev Res (Phila) 3:1148-1156

FIGURE LEGENDS

Figure 1: *c-JUN* expression in non-COPD and COPD lung tissues. (A) Real-time analysis of c-JUN mRNA levels in non-COPD (n=21), moderate-COPD (n=24) severe COPD (n=13) and very severe COPD (n=30) human lung tissue biopsies. The horizontal and vertical lines were plotted as median ± interquartile range. Linear regression analysis was performed without any adjustment and with further adjustment for sex, age and cigarette pack-years. *P = 0.008, non-COPD vs very severe-COPD. One-way ANOVA with Bonferroni corrections was performed for multiple group comparisons. **P = 0.05, non-COPD vs very severe-COPD. **(B)** Immunoblot analyses of c-JUN in non-COPD, severe-COPD and very severe-COPD lung homogenates (left panel). Immunoblot analysis of c-JUN in non-COPD and moderate-COPD was shown in right panel. β-actin was used as reference for loading control. c-JUN protein bands were quantified and normalized to β-actin in each sample using Bio-Rad Image Lab software. The horizontal and vertical lines were plotted as median ± interquartile range for each group (n=9). Linear regression analysis was performed without any adjustment and with further adjustment for sex, age and cigarette pack-years. *P = 0.001, non-COPD vs very severe-COPD or moderate-COPD vs very severe-COPD. One-way ANOVA with Bonferroni corrections was performed for multiple group comparisons. **P = 0.001, non-COPD vs very severe-COPD or moderate-COPD vs very severe-COPD. **(C)** Immunohistochemical analysis of c-JUN on lung sections of non-COPD, moderate-COPD, severe-COPD and very severe-COPD patients. Graph represents the number of c-JUN positive cells. One-way ANOVA with Bonferroni corrections was performed for multiple group comparisons.*P = 0.001, Non-COPD vs severe-COPD and very severe-COPD; or moderate-COPD vs severe-COPD and very severe-COPD.

Figure 2: Deletion of c-Jun induces inflammation and emphysema in mice. Mice

(n= 8) were sacrificed at the age of 1.5, 3, 8 or 12 months. Lungs were inflated and fixed in 1.5% paraformaldehyde. Lung sections (5μ) were prepared and stained with H & E. **(A)** Lung images (400x) of 1.5, 3, 8 or 12 months old *c-Jun*$^{f/f}$ and *c-Jun*$^{\Delta ae}$ mice were shown. Arrows indicate the presence of foamy macrophages. Bottom panel represents 40x images of the lungs of *c-Jun*$^{\Delta ae}$ and *c-Jun*$^{f/f}$ mice at 12 months of age. **(B)** Serial images of H & E stained lung sections (100x) were taken and then mean chord lengths (MCL) were measured using computer-assisted morphometry with Image Pro Plus software. The values represented are mean MCL ± SEM. One-way ANOVA followed by Newman-Kuels post hoc analysis was performed for multiple group comparisons, whereas two-way ANOVA with a Bonferroni correction was used for comparing the interaction between genotype and age. In both cases *P* values with ≤ 0.05 were considered as statistically significant. *$P \leq 0.05$ *c-Jun*$^{f/f}$ vs *c-Jun*$^{\Delta ae}$.

Figure 3: c-Jun deficiency leads to DNA damage. TUNEL staining was performed on lung tissues obtained from *c-Jun*$^{f/f}$ and *c-Jun*$^{\Delta ae}$ mice (n=3) using In Situ Cell Death Detection Kit. Nuclei were stained with propidium iodide. **(A)** Images of the TUNEL stainings of 1.5, 3, 8 or 12 month old mice (200x) were shown. TUNEL-positive epithelial cells and macrophages were indicated with white arrows and asterisks, respectively. **(B)** TUNEL-positive epithelial cells were counted (10 fields/lung sections) and the averages of 3 mice ± SEM were given. * $P \leq 0.05$, 1.5 M old vs other age groups; †$P \leq 0.05$, *c-Jun*$^{f/f}$ *vs c-Jun*$^{\Delta ae}$ mice.

Figure 4: Expression levels of antioxidant enzymes and inflammatory cytokines. **(A)** Total RNA was isolated from the lungs of 1.5, 3, 8 or 12 month old *c-Jun*$^{f/f}$ and *c-Jun*$^{\Delta ae}$ mice and cDNA was prepared. The expression levels of Gclc, Nqo1 and Hmox1

were determined using Taqman gene real time probes. Significance was calculated using student's "*t*' test. *$P \leq 0.05$, *c-Jun*$^{f/f}$ vs *c-Jun*$^{\Delta ae}$ mice. **(B)** Cytokines were measured in BAL fluids of 1.5, 3, 8, or 12 month-old *c-Jun*$^{f/f}$ and *c-Jun*$^{\Delta ae}$ mice. Cytokines analyses were performed with multiplex suspension array system using Luminex beads. The mean values of cytokines in picograms $\pm$ SEM of IL-12p40, IL-13, Cxcl1 (KC) and TNF-α were given (n=5). Significance was calculated using student's "*t*' test. *$P \leq 0.05$, *c-Jun*$^{f/f}$ vs *c-Jun*$^{\Delta ae}$ mice.

Figure 5: Cigarette smoke induced inflammation and emphysema in the lungs of *c-Jun*$^{f/f}$ and *c-Jun*$^{\Delta ae}$ mice. Mice were exposed to cigarette smoke (CS) or filtered room air (RA) for 6 months. BAL was collected from the right lung, centrifuged, and stained with Diff-Quik stain kit. Left lung was inflated with 0.8% agarose and fixed in 1.5% paraformaldehyde. **(A)** Differential cell counts were performed and expressed as mean $\pm$ SEM for total cells, neutrophils, macrophages and lymphocytes. One-way ANOVA followed by Newman-Kuels post hoc analysis was performed for multiple group comparisons, whereas two-way ANOVA with a Bonferroni correction was used for comparing the interaction between genotype and CS. In both cases *'P'* values with $\leq$ 0.05 were considered as statistically significant. **P* $\leq$ *0.05* filtered air vs cigarette smoke; †*P* $\leq$ 0.05, *c-Jun*$^{f/f}$ vs *c-Jun*$^{\Delta ae}$ mice. **(B)** Histopathology of lung sections showing the perivascular and peribronchial cellular infiltrate. Lung sections were prepared from mice exposed to RA and CS and stained with H & E. **(C)** Serial images of H & E stained lung sections (100x) of *c-Jun*$^{f/f}$ and *c-Jun*$^{\Delta ae}$ mice exposed to CS and RA were taken and then mean chord lengths (MCL) were measured using computer-assisted morphometry with Image Pro Plus software. The values represented are mean MCL $\pm$ SEM. One-way ANOVA followed by Newman-Kuels post hoc analysis was performed for multiple group comparisons, whereas two-way ANOVA with a Bonferroni correction was used for

comparing the interaction between genotype and CS. In both cases *P* values with $\leq$ 0.05 were considered as statistically significant.* $P \leq 0.05$ RA vs CS exposed mice. **(D)** The tissue sections obtained from the lungs of mice exposed to CS or RA were immunostained with anti-CD3 antibodies **(E)** and anti-B220 antibodies. Graphs represent the c-Jun positive T and B lymphocytes.

Table 1. Clinical and Demographic characters of the Study Population.

Parameters	Non-COPD	Moderate-COPD	Severe-COPD	Very severe-COPD
Age (Mean ± SD)	63.1 ± 11.5	69.4 ± 8.2	64.9 + 7.9	55.2 + 5.8
Sex				
M	11	13	7	14
F	10	11	6	16
Smoking Status				
Current	1	4	2	0
Ever	14	17	11	28
Never	6	1	0	1
Not Known	0	2	0	1
Packs/year (Mean +SD)	43.8 + 40.4	45.8 ± 24.5	34.8 + 21.6	46.3 + 33.1
Pulmonary Function Parameters				
FEV1 (Mean ± SD)	91.5 ± 8.2	62.7+10.4	36.9 + 5.3	18.0 + 4.0
FCV (Mean ± SD)	95.1 ± 9.2	77.1+ 15.7	62.2 + 15.4	47.1 + 14.1
Gold stage - 0/I/II/III/IV	14/7/0/0/0	0/0/24/0/0	0/0/0/13/0	0/0/0/0/30

Values represent the number of patients or mean ± SD. Gold = Global Initiative for Chronic Obstructive Lung Disease.

Figure 1

A

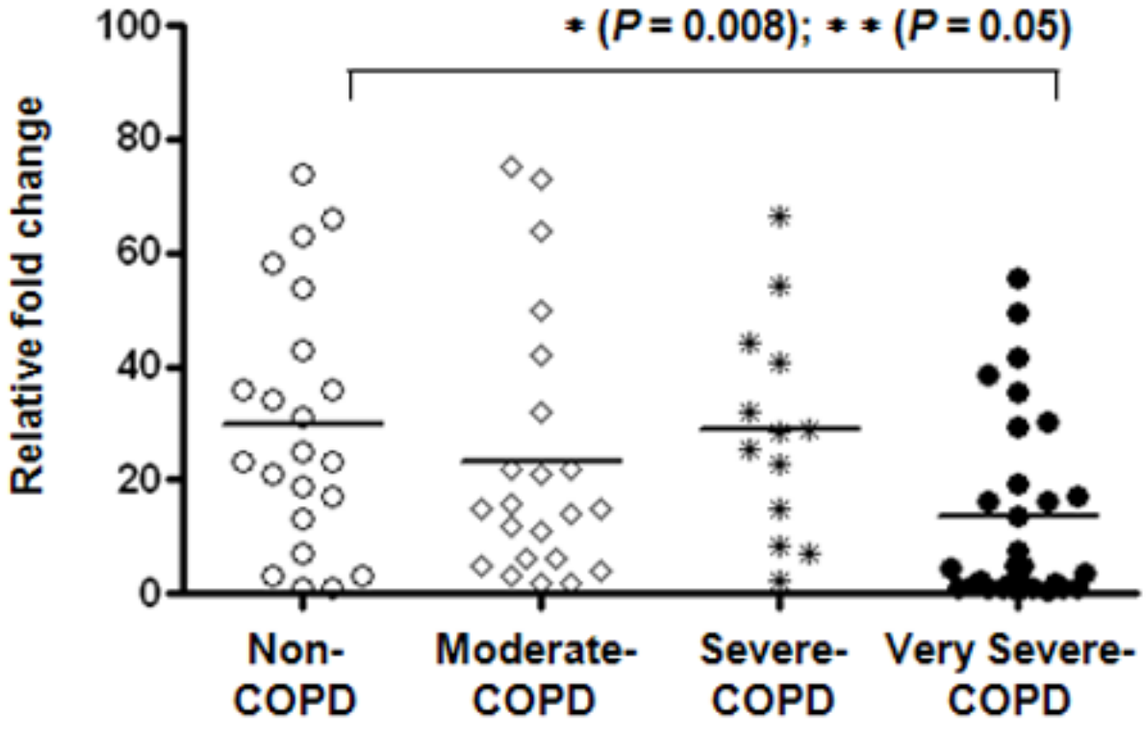
* (P = 0.008); * * (P = 0.05)
Relative fold change
100
80
60
40
20
0
Non-COPD
Moderate-COPD
Severe-COPD
Very Severe-COPD

B

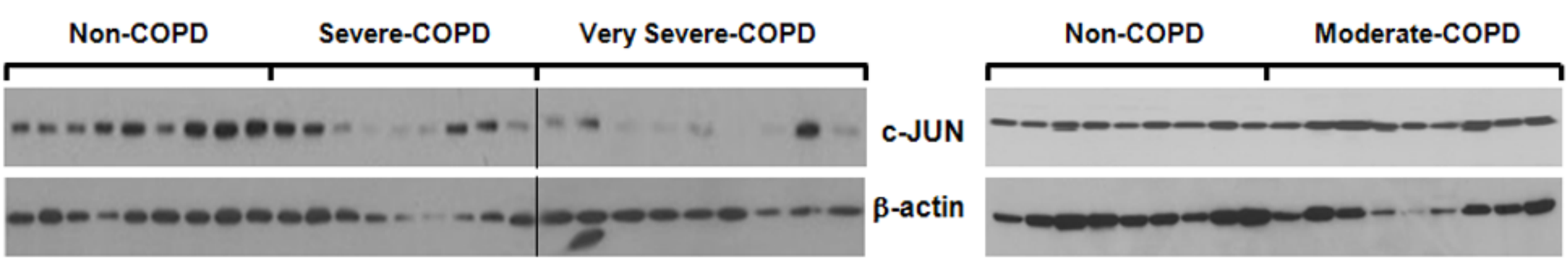
Non-COPD
Severe-COPD
Very Severe-COPD
Non-COPD
Moderate-COPD
c-JUN
β-actin

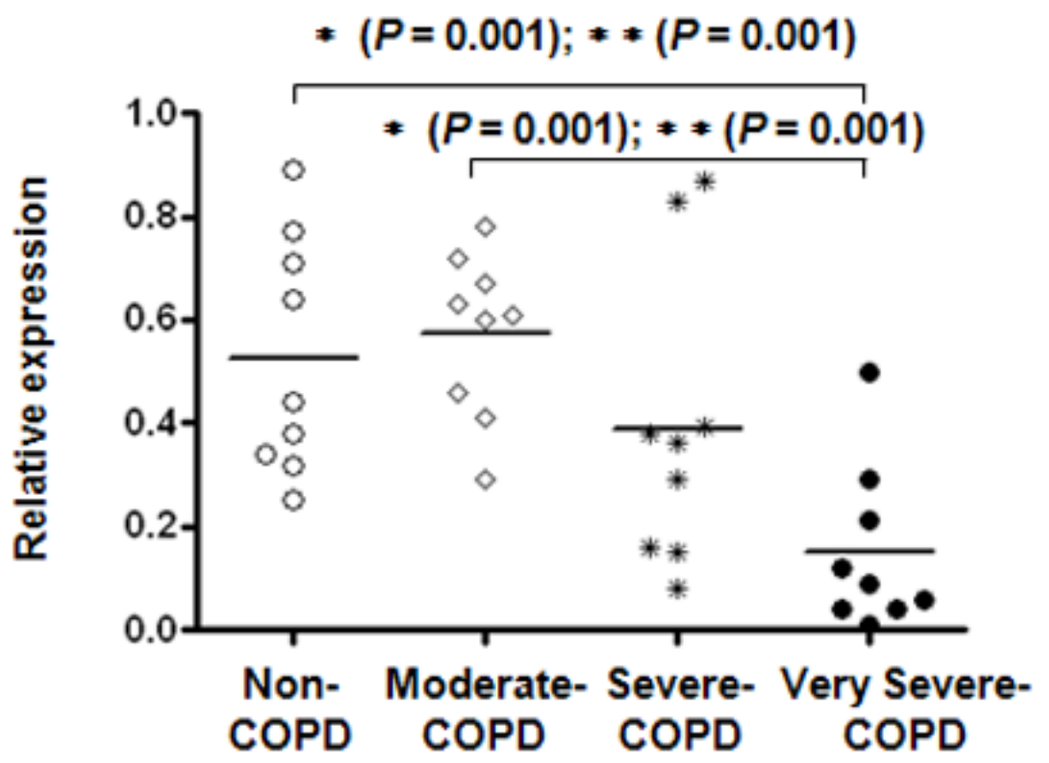
* (P = 0.001); * * (P = 0.001)
* (P = 0.001); * * (P = 0.001)
Relative expression
1.0
0.8
0.6
0.4
0.2
0.0
Non-COPD
Moderate-COPD
Severe-COPD
Very Severe-COPD

C

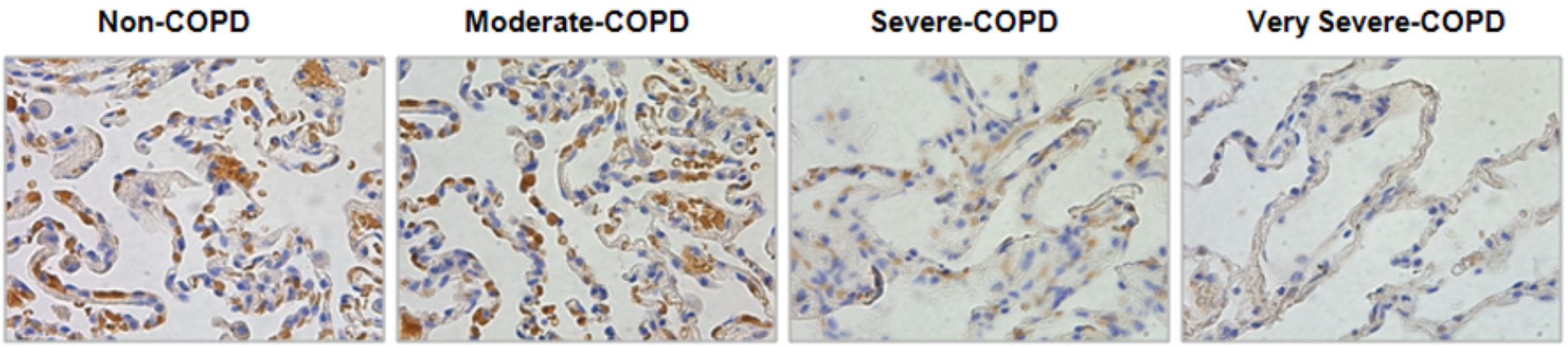
Non-COPD
Moderate-COPD
Severe-COPD
Very Severe-COPD

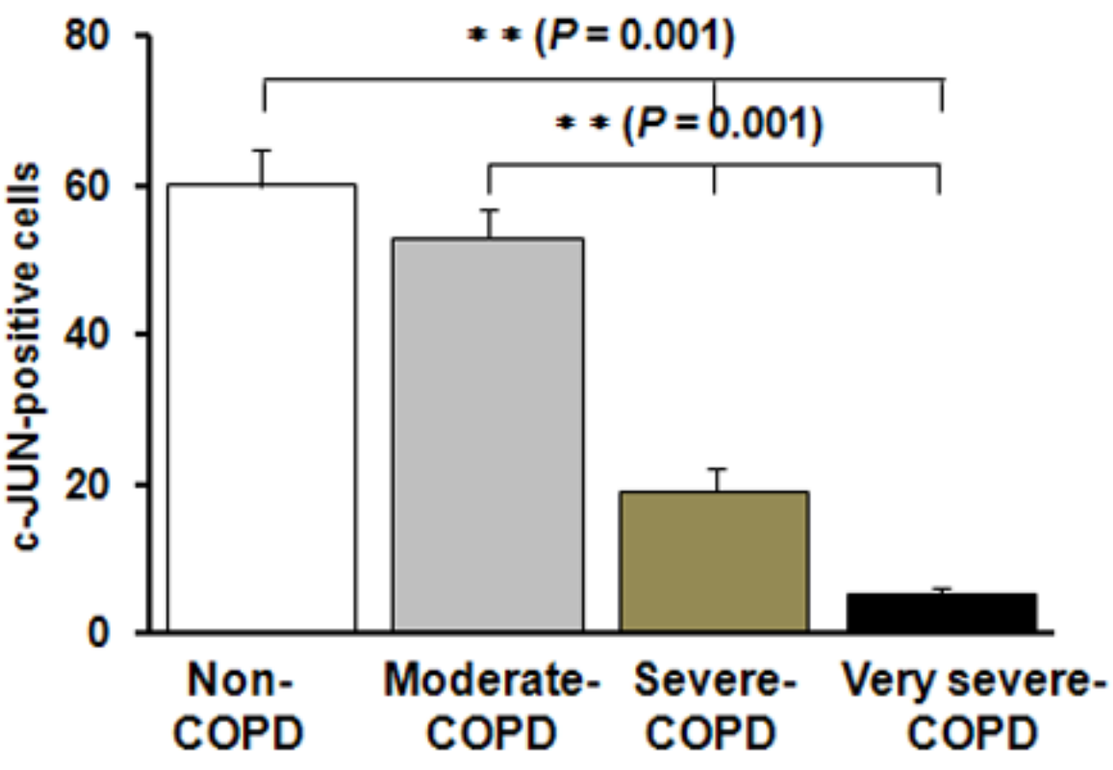
* * (P = 0.001)
* * (P = 0.001)
c-JUN-positive cells
80
60
40
20
0
Non-COPD
Moderate-COPD
Severe-COPD
Very severe-COPD

Figure 2

A

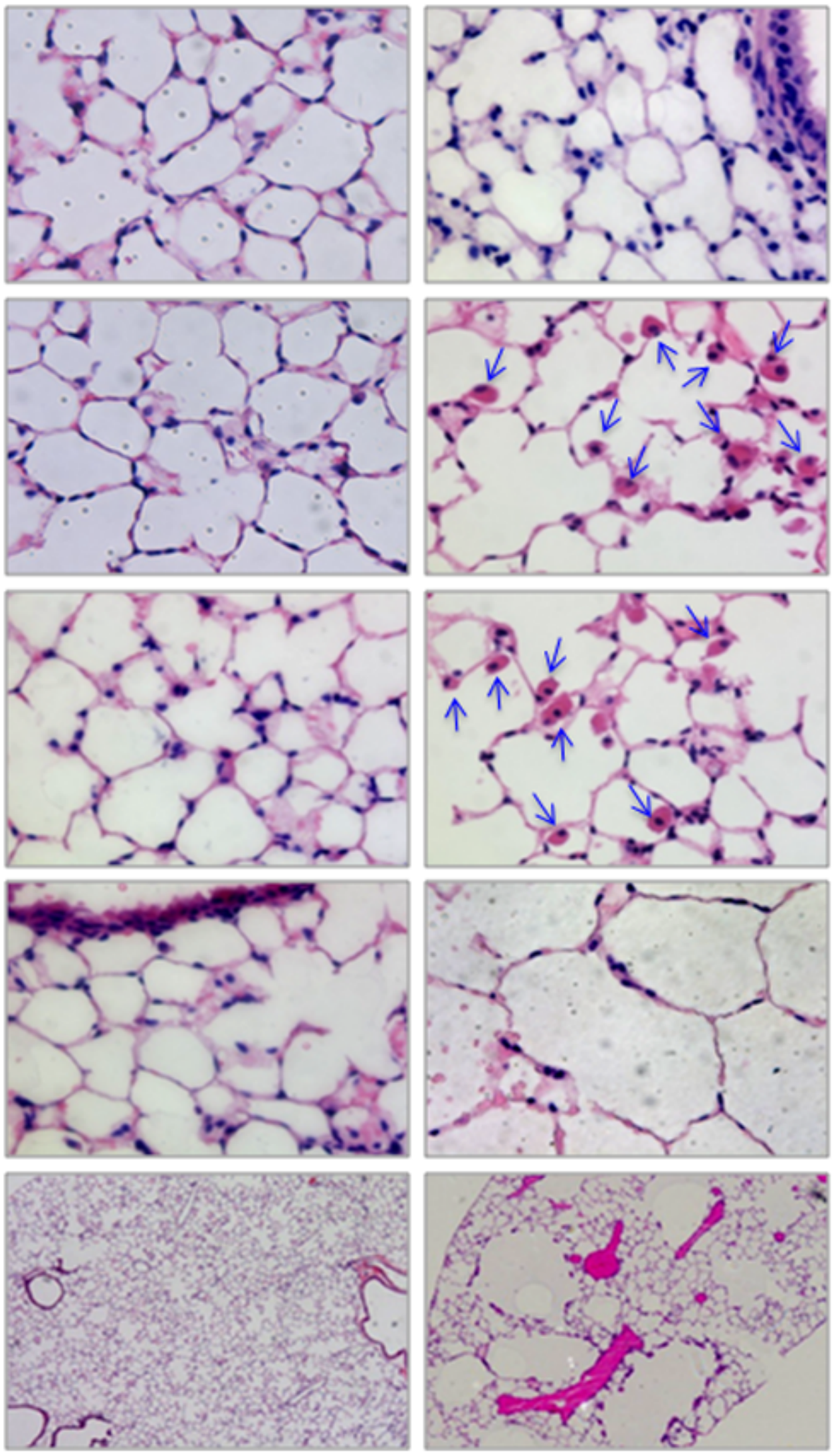
c-Jun^f/f
c-Jun^Δae
1.5 M (400x)
3 M (400x)
8 M (400x)
12 M (400x)
12 M (40x)

B

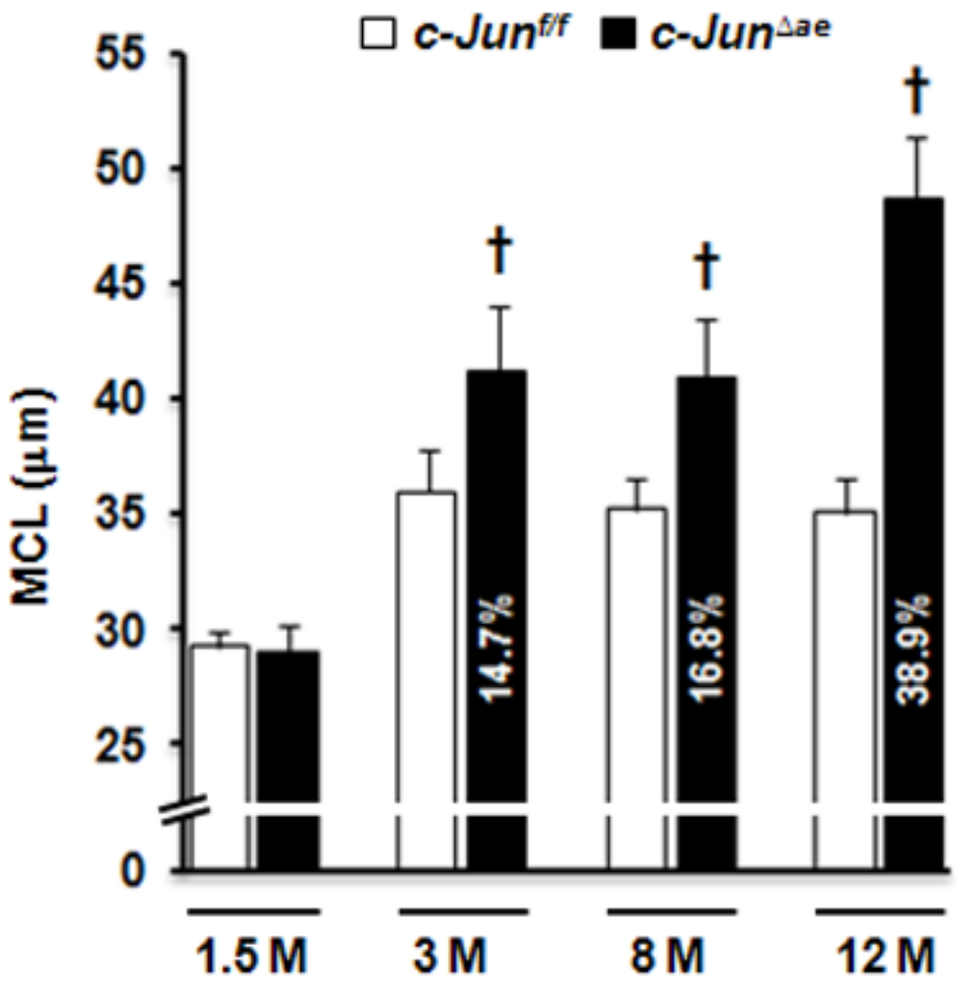
c-Jun^f/f
c-Jun^Δae
MCL (µm)
55
50
45
40
35
30
25
0
†
†
†
14.7%
16.8%
38.9%
1.5 M
3 M
8 M
12 M

Figure 3

A

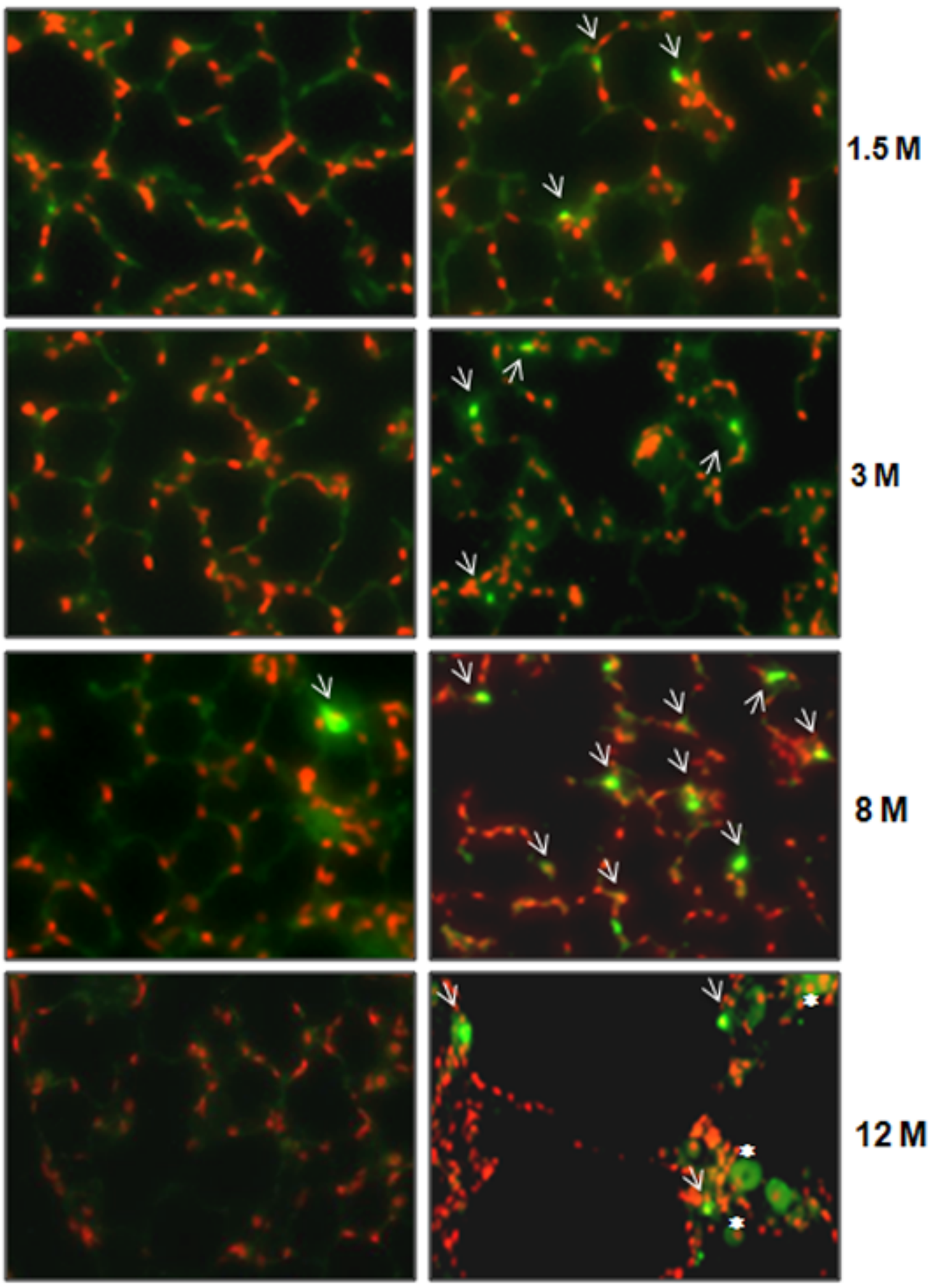
c-Jun f/f
c-Jun Δae
1.5 M
3 M
8 M
12 M

B

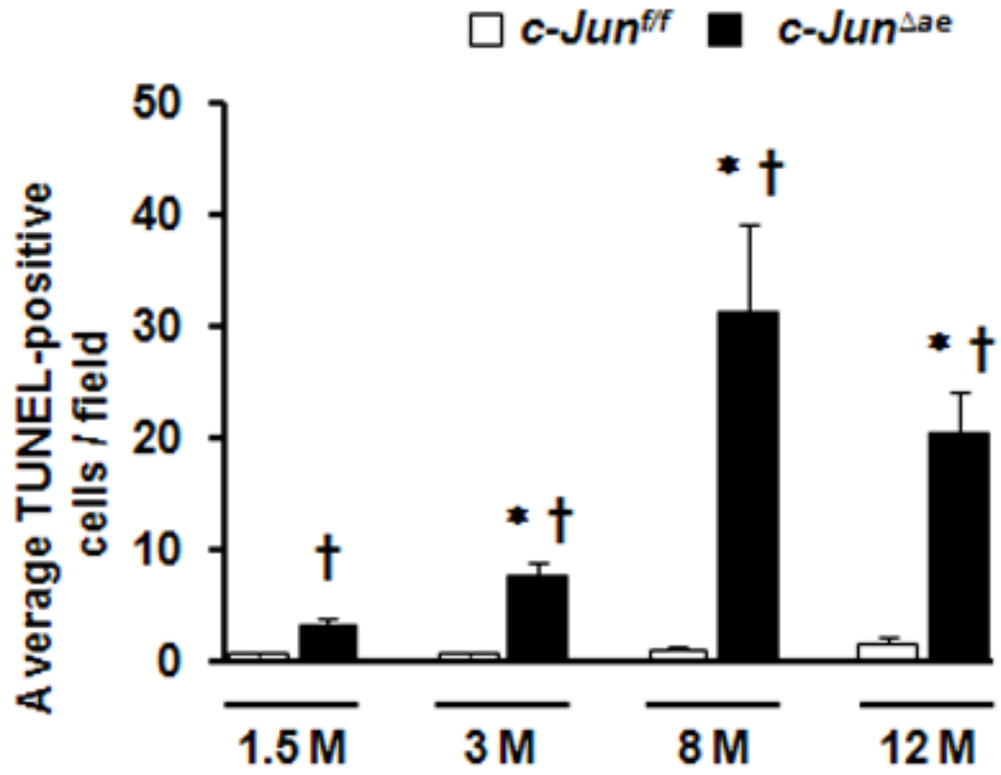
c-Jun f/f
c-Jun Δae
Average TUNEL-positive cells / field
50
40
30
20
10
0
1.5 M
3 M
8 M
12 M

Fig. 4

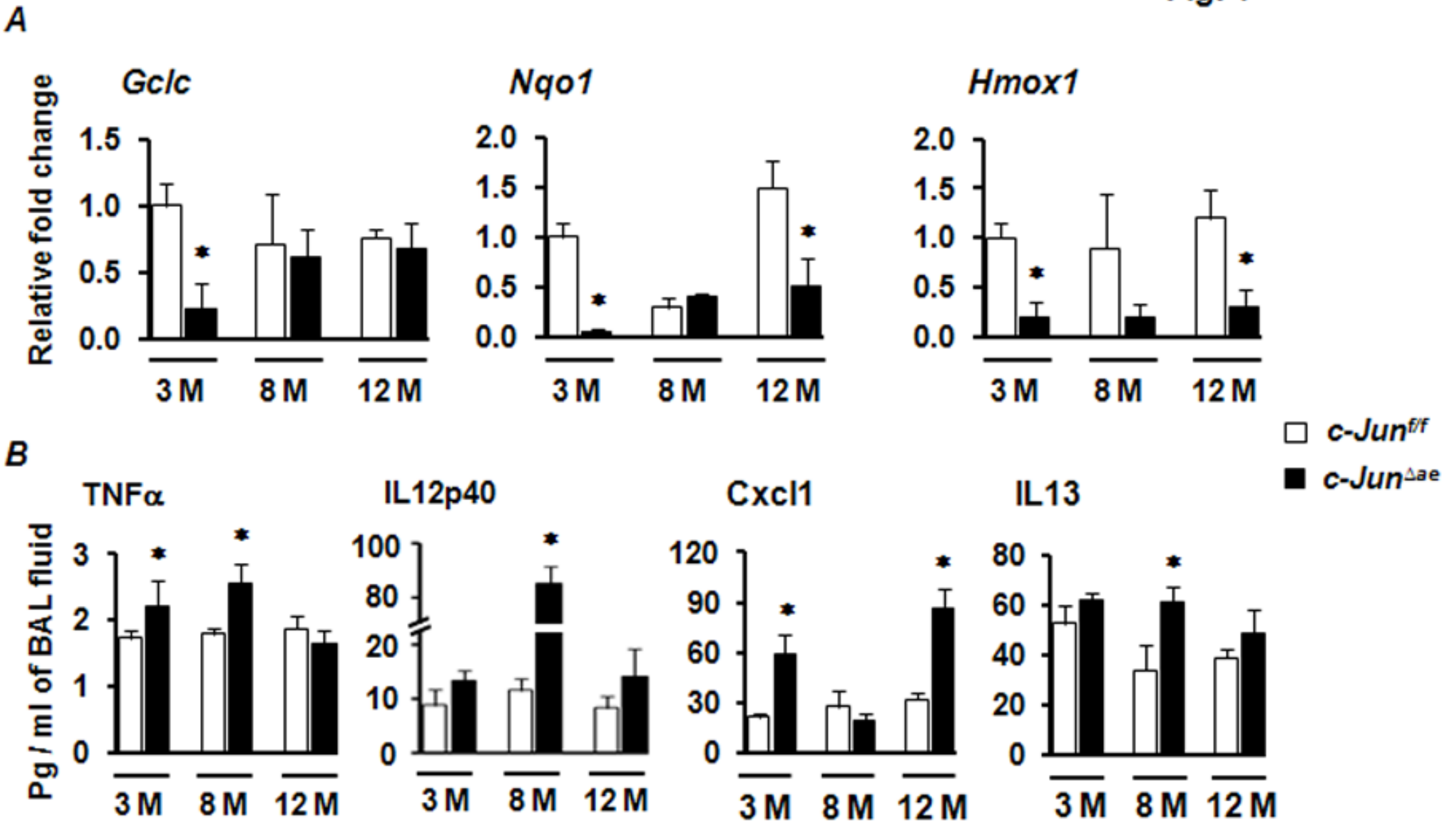
A
Gclc
Nqo1
Hmox1
Relative fold change
1.5
1.0
0.5
0.0
2.0
1.5
1.0
0.5
0.0
2.0
1.5
1.0
0.5
0.0
3 M
8 M
12 M
3 M
8 M
12 M
3 M
8 M
12 M
c-Jun f/f
c-Jun Δae
B
TNFα
IL12p40
Cxcl1
IL13
Pg / ml of BAL fluid
3
2
1
0
100
80
20
10
0
120
90
60
30
0
80
60
40
20
0
3 M
8 M
12 M
3 M
8 M
12 M
3 M
8 M
12 M
3 M
8 M
12 M

Figure 5

A

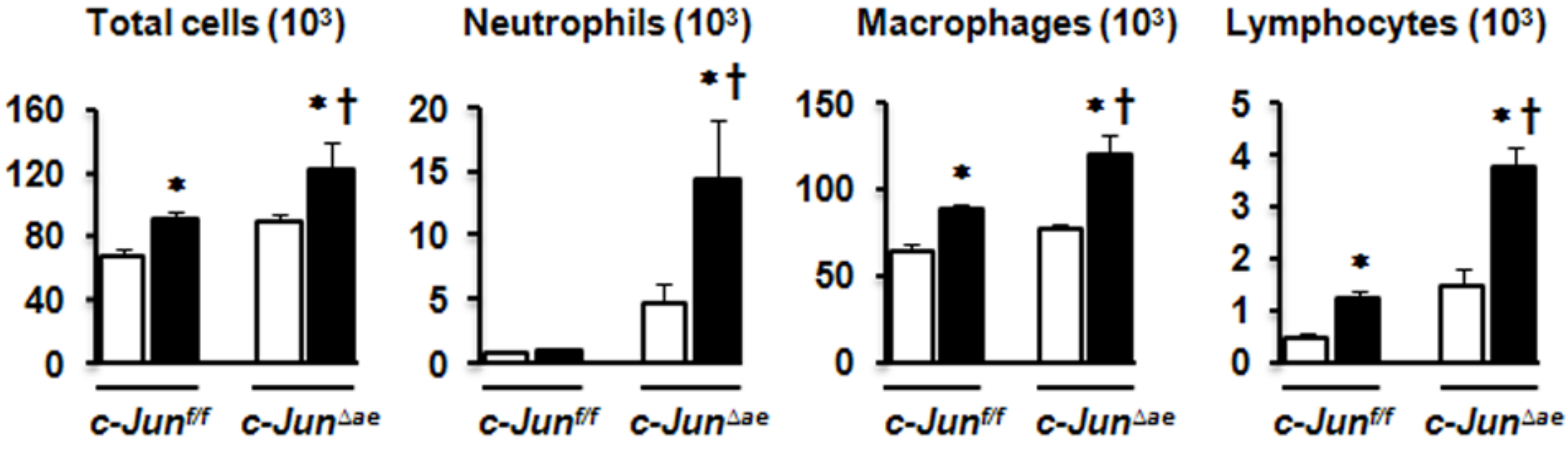

B

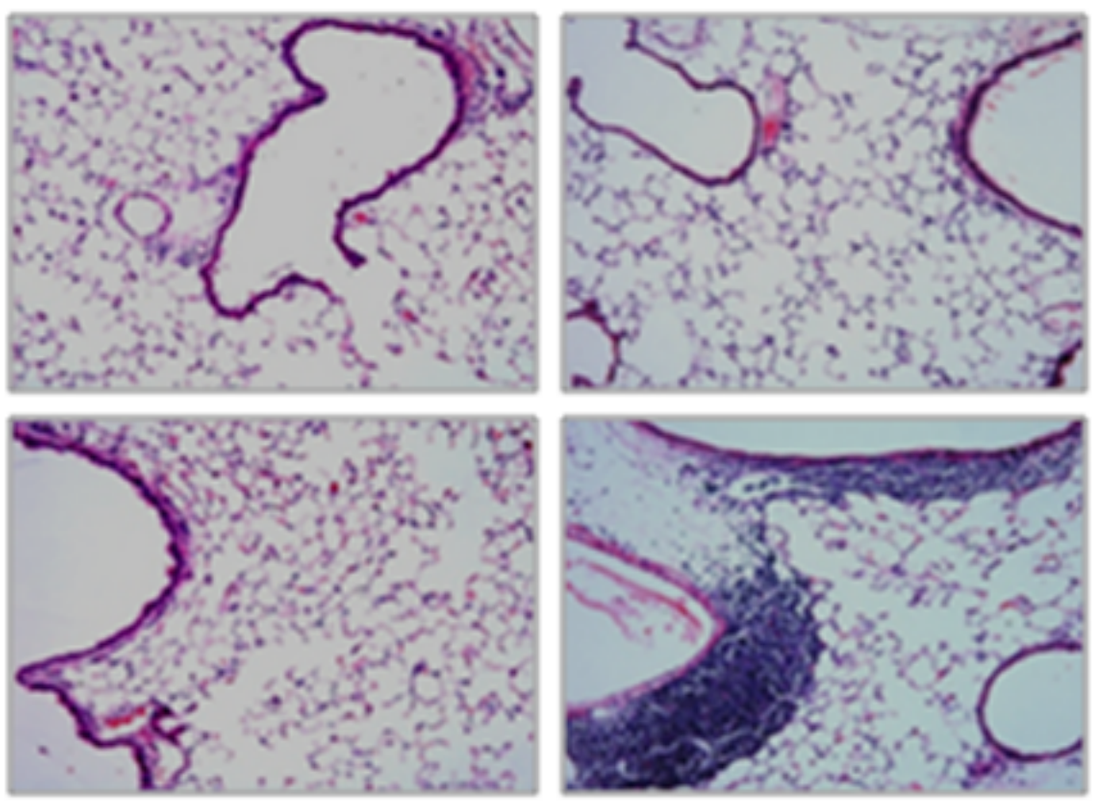

C

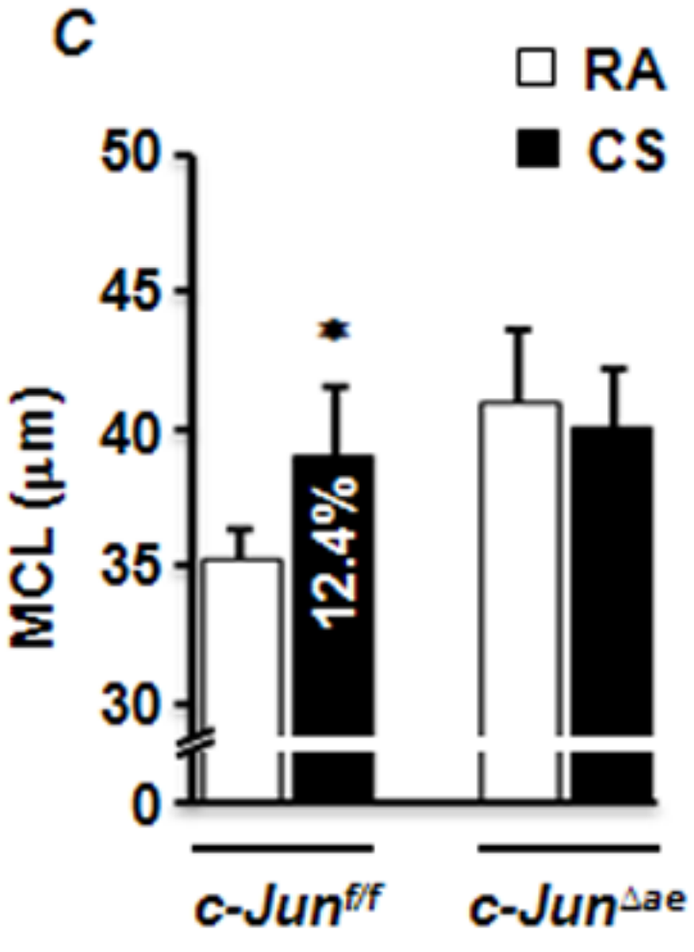

D

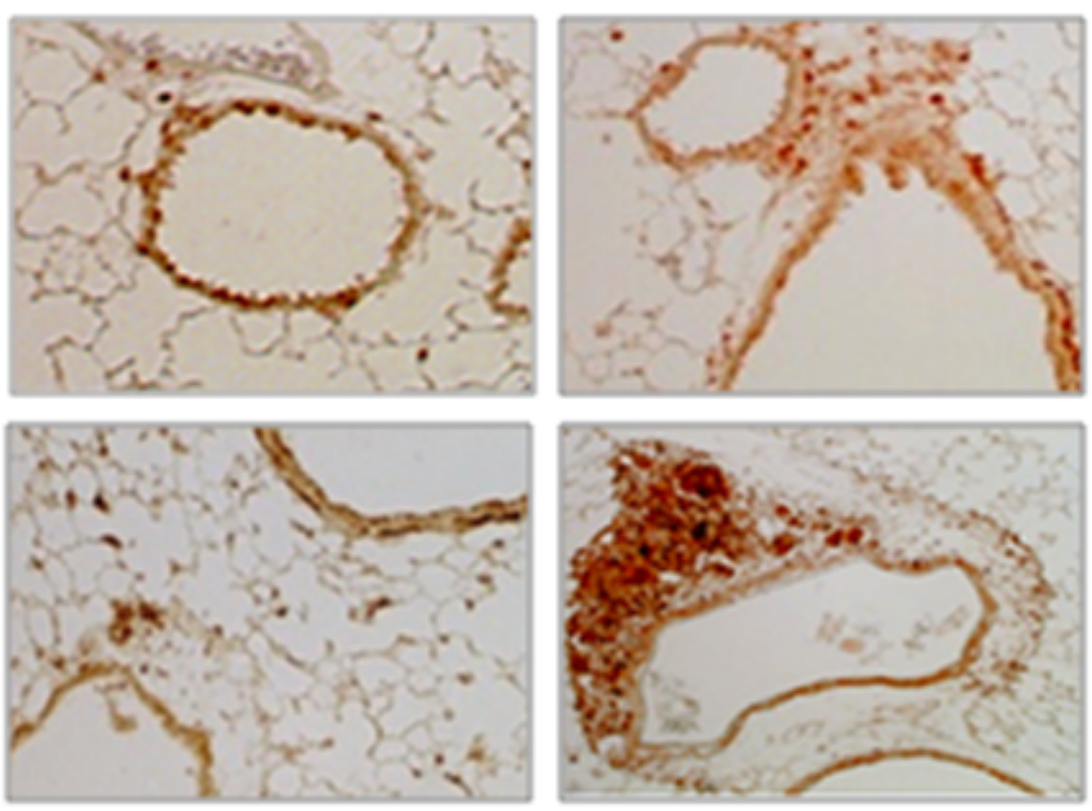

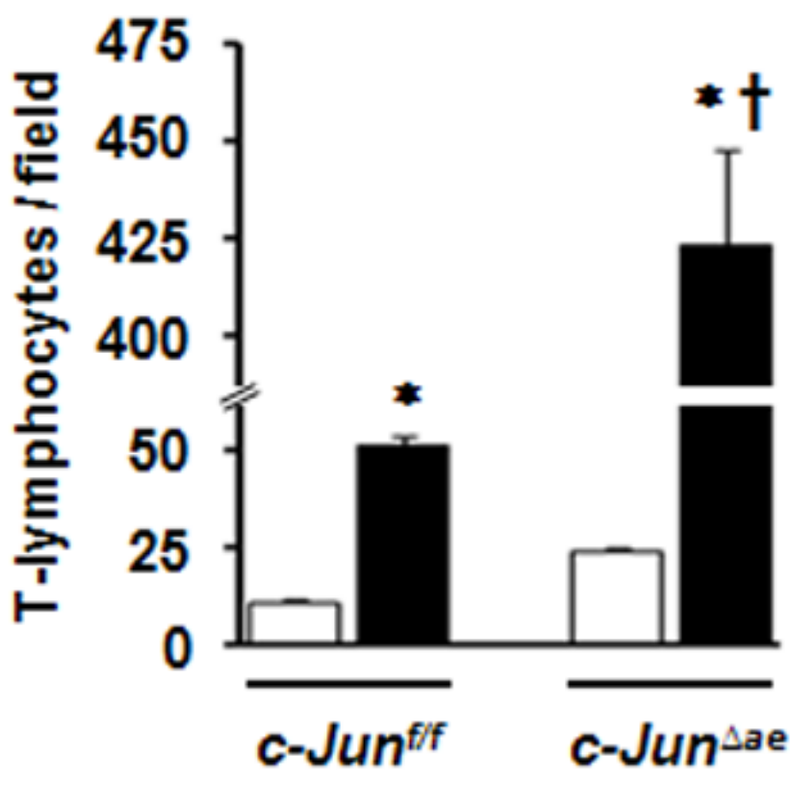

E